LIGHT EMISSION FROM WATER IRRADIATED WITH HIGH ENERGY ELECTRONS

by

ERIC ALBERT SHAEDE

B.Sc., University of British Columbia, 1966

A THESIS SUBMITTED IN PARTIAL FULFILMENT OF THE REQUIREMENTS FOR THE DEGREE OF MASTER OF SCIENCE

in the Department of Chemistry

We accept this thesis as conforming to the required standard.

THE UNIVERSITY OF BRITISH COLUMBIA

October, 1967

In presenting this thesis in partial fulfilment of the requirements for an advanced degree at the University of British Columbia, I agree that the Library shall make it freely available for reference and study. I further agree that permission for extensive copying of this thesis for scholarly purposes may be granted by the Head of my Department or by his representatives. It is understood that copying or publication of this thesis for financial gain shall not be allowed without my written permission.

Department of Chemistry
The University of British Columbia
Vancouver 8, Canada
October 11, 1967.

ABSTRACT

Luminescence has been observed from water irradiated with an intense pulse of high energy electrons. The angular dependence, electron energy dependence, visible spectrum, lifetime and yield of the light emission have been determined. In addition, the effect of additives on the emission was studied. The emission spectrum of water was found to be identical to that of methanol, cyclohexane and benzene. All of these results lead to the conclusion that no light emission other than Cerenkov radiation was present in the visible region of the spectrum. The yield of Cerenkov radiation was found to be $G_{h\nu(4\text{-}5000\,\text{Å})} \sim 6 \times 10^{-4}$.

TABLE OF CONTENTS

	PAGES
INTRODUCTION	
1. Radiation Chemistry	1-9
(a) The Interaction of Ionizing Radiation with matter	1-5
(i) Electrons	1-3
(ii) Electromagnetic Radiation	3-5
(b) General Radiation Chemistry of the Liquid Phase	5-7
(i) Chemical Effects of the Radiation	5-6
(ii) Linear Energy Transfer	6-7
(iii) Absorbed Dose	7
(iv) G-values	7
(c) Radiation Chemistry of Liquid Water	8-9
2. Cerenkov Radiation	9-14
3. Previous Investigations of Light Emission from Irradiated Water	14-16
4. Scope of the Present Investigation	16-18
EXPERIMENTAL	
1. Electron Accelerator	19
2. Electron Beam Current Measurements	20-21
3. Dosimetry	21-22
4. Spectral Analysis Systems	23-29
(a) Photomultiplier-Interference Filter Wedge Spectrometer	23-27
(b) Grating Spectrograph	27-29
5. Densitometry	29

	PAGES
6. 180° Camera	29-30
7. Irradiation Cell and Water Flow System	30-31
8. Actinometry	31-32
9. Spectrofluorimetry	32
10. Materials	32-33
(a) Water	32
(b) Scintillator	32
(c) Photographic Materials	33
(d) Other Materials	33
11. Electrical Noise	33
RESULTS AND DISCUSSIONS	
1. Preliminary Investigations	34
2. The Angular Dependence of the Light Emission	35-36
3. Variation of the Emission Intensity with Electron Energy	37-38
4. The Emission Lifetime	39
5. Actinometry	40
6. The Emission Spectrum	41
(a) Photomultiplier-Interference Filter Wedge Spectrometer	41
(b) Grating Spectrograph	43-44
7. The Effect of Additives	45-46
8. Comparison of Water with other Liquids	47-49
9. Calculation of a G-value	50-51
10. Conclusions	52
11. Suggestions for Further Study	53-54
REFERENCES	
ILLUSTRATIONS	

LIST OF ILLUSTRATIONS

Figure 1: Diagram showing the constructive interference of Cerenkov radiation by Huygens construction.

Figure 2: Field Emission Electron Accelerator photograph.

Figure 3: (a) Electron beam pulse shape (b) Light emission from water pulse shape (c) Light emission from scintillator pulse shape.

Figure 4: Faraday cup and aperture; photograph and diagram.

Figure 5: Electron beam current as a function of accelerator charging voltage.

Figure 6: Photomultiplier-interference filter wedge spectrometer, (a) photograph (b) diagram

Figure 7: Experimental setup diagram showing apparatus layout.

Figure 8: The spectral sensitivity of the photomultiplier-interference filter wedge spectrometer.

Figure 9: The grating spectrograph; photograph and diagram.

Figure 10: Spectral sensitivity of the grating spectrograph with HP4 film.

Figure 11: 180° Camera; photograph and diagram.

Figure 12: Stainless steel irradiation cell; photograph and diagram.

Figure 13: Angular dependence of the light emission from (a) water, (b) quartz and (c) scintillator. ΔD as a function of θ.

Figure 14: The peak intensity of the light emission from (a) water and (b) scintillator as a function of charging voltage of the accelerator.

Figure 15: The peak intensity of the light emission from (a) water and (b) scintillator divided by the product of electron beam peak current and energy as a function of charging voltage of the accelerator. (Int./ExI vs charging voltage).

Figure 16: The peak intensity of the light emission from water divided by the peak electron beam current as a function of $1(1-1/\beta^2 n^2)$.

Figure 17: The emission spectrum of water as determined with the photomultiplier-spectrometer.

Figure 18: The emission spectrum of the scintillator as determined by (a) the photomultiplier-spectrometer (b) the spectro-photofluorometer.

Figure 19: The emission spectrum of water as determined with the grating spectrograph.

Figure 20: The densitometer tracings of the emission bands of (a) water (b) methanol (c) cyclohexane (d) benzene as determined with the grating spectrograph.

I wish to thank Dr. D.C. Walker for his assistance both in the laboratory and in the writing of this thesis. His comments and criticism were of extreme value.

I am indebted to Mr. Dick Espejo of Field Emission Corporation, who provided technical assistance and information on the operation of the accelerator.

I am grateful to Dr. A. Bree for use of his microdensitometer, Dr. E.A. Ogryslo for the loan of his grating spectrograph and Dr. G. Porter for the use of his calibrated quartz-iodine lamp.

INTRODUCTION

1. Radiation Chemistry

(a) The Interaction of Ionizing Radiation with Matter

"Some knowledge of the processes by which radiation interacts with matter is essential to an understanding of radiation chemical phenomena, since the chemical effects are a direct consequence of the absorption of energy from the radiation".[1]

(i) Electrons

The interaction of electrons with matter occurs by three important processes, (i) radiation emission (Bremsstrahlung), (ii) inelastic collisions and (iii) elastic collisions, the latter essentially resulting only in a change of direction of motion of the electron. The relative importance of these processes depends upon the electron energy.

As a high speed charged particle passes in the vicinity of a nucleus it may be decelerated by the electric field and will therefore radiate electromagnetic energy (Bremsstrahlung) in order that the system may conserve both energy and momentum. The rate at which this energy loss occurs, $-dE/dx$, is proportional to Z^2z^2/m^2, where z,Z are the charges on the particle and nucleus respectively and m is the mass of the particle. For electrons, Bremsstrahlung emission is negligible below 100 keV. and becomes predominate in the energy range 10-100 Mev.

Energy loss can also occur by coulomb interactions with

the electrons of the stopping material. Interactions of this type, or inelastic collisions, produce ionization and excitation in the medium and is the dominant form of energy loss by electrons having energies less than 1 MeV.

The third process of interaction of electrons with matter, elastic scattering, is a result of the deflection of the electron by the coulomb potentials of the atomic nuclei of the medium. Elastic scattering is important for low energy electrons and high atomic number materials.

Thus electrons lose their energy and are defected as they pass through a material. The rate of energy loss and the total initial energy consequently determine the range or penetration distance of the electron in a given material. For monoenergetic electrons, a graph showing the number of electrons at a certain distance within the bombarded material as a function of distance is nearly linear with a negative slope and finishing in a small tail. The extrapolated or practical range, Rp, is found by extrapolating the near linear portion of the curve. The maximum range, R_o, is the point where the tail of the curve merges with the background. For nonmonoenergetic beams, or β-rays, the curve does not have a linear region and only a maximum range, R_o, can be determined. An empirical formula can be used to relate the energy of the electrons to their range in aluminum (and most other light elements since the range varies only slightly with atomic number). For energies in the range 0.01 - 2.5 MeV. the maximum

range of β-rays or the extropolated range for monoenergetic electrons is given by[2]

$$\text{Range } (mg/cm^2) = 412\ E^{1.265-0.0954\ln E} \qquad (i)$$

where E is the maximum energy of the β-rays or the energy of the monoenergetic electrons.

(ii) Electromagnetic Radiation

In contrast to charged particles, which have a definite maximum range in a medium, X or γ-rays obey absorption laws common to other electromagnetic radiations. Thus X or γ-rays are incompletely absorbed by a finite thickness of absorbing material. The reduction in intensity, dI, of the incident beam of X or γ-rays on passing through an increment of matter of thickness, dx, is given by[2]

$$dI = Io\ \mu\ dx \qquad (ii)$$

where μ is the linear absorption coefficient of the material and Io is the incident intensity of the radiation. The total linear absorption coefficient, μ, is a sum of the partial coefficients representing the various processes involved in the absorption. The three most important absorption processes are (i) the photoelectric process, (ii) the Compton effect and (iii) pair production. The relative importance of these processes is governed by the energy of the photon and the electron density of the stopping material.

The photoelectric effect is the interaction of the electromagnetic radiation with an atom or molecule which results in the complete absorption of the photon and simultaneous ejection

of an electron with kinetic energy, E_e, given by[2]

$$E_e = h\nu - E_o \qquad \text{(iii)}$$

where E_o is the binding energy of the electron and $h\nu$ is the energy of the photon. This process is predominant for low photon energies (< 0.5 MeV) and high atomic number materials.

The interaction of a photon with an electron of the medium by the Compton effect results in a scattering of the photon and transfer of some energy to the electron. The energy of the recoil electron, E_e, is given by[2]

$$Ee = h\nu - h\nu' \qquad \text{(iv)}$$

where $h\nu$ and $h\nu'$ are the incident and scattered photon energies respectively. E_e varies from zero to a certain maximum, and its value depends on the angular relationship of the collision and the scattered photon. The maximum energy of the Comption electron, E max, is given by[3]

$$E\ max = \frac{E_o}{1 + 0.25/E_o} \qquad \text{(v)}$$

where E_o is the energy of the incident photon. This process is dominant at medium photon energies (1 - 10 MeV) and in high electron density materials.

Pair production is the result of the annihilation of a photon in the region of an atomic nucleus with the concomitant production of an "electron" pair - a positive and a negative electron. This process has a threshold energy of 1.02 MeV. which is required to produce the two electron rest masses. The kinetic energies of the "electrons", Ep and Ee, are given by[2]

$$Ep + Ee = h\nu - 2m_oc^2 = h\nu - 1.02\ MeV \qquad \text{(vi)}$$

where $h\nu$ is the photon energy. This process becomes predominate at high photon energies (> 10 MeV).

Hence when X or γ-rays are absorbed in a medium, high energy electrons are generated which then dissipate their energy by the processes discussed in section (i).

(b) General Radiation Chemistry of the Liquid Phase

(i) Chemical Effects of the Radiation

The chemical effects following the absorption of radiation are a result of the ionizations and excitations caused by the high speed primary electron (or Compton electron in the case of X or γ-ray irradiations) and its secondary electrons. The path of the primary electron is refered to as a track and it is generally linear at high energies but deflections become more common as the electron energy decreases. Secondary ionizations along the track result in two types of secondary electrons, the low energy secondary ($< \sim 100$ eV.) and the high energy secondary ($> \sim 100$ eV.). The low energy secondary electrons will undergo wide deflections and form a region of tertiary ionization and excitation, known as a spur, which may, to a first approximation, be regarded as spherical. The high energy secondary electron will form a short track of its own, known as a δ-ray, with a number of spurs along it.

Each spur contains a number of excited molecules, positive ions, and electrons. Following their formation, which takes

about 10^{-16} seconds, these species may undergo various transformations in the physiochemical stage of the radiolysis. These processes, which include ion-molecule reactions, electron capture, dissociation of excited molecules, energy transfer and solvation of electrons, occur in a time of about 10^{-10} seconds. The chemical stage of the radiolysis occurs during times longer than 10^{-10} seconds and consists of the formation of molecular products by radical-radial, radical-ion or ion-ion reactions within the spurs, the formation of products from radical-solute or radical-solvent reactions following the diffusion of radicals and molecular products from the spurs and the de-excitation of electronically excited molecules by fluorescence, phosphorescence or quenching.

(ii) Linear Energy Transfer (L.E.T.)

The spacial distribution of the spurs formed by the radiation determines the yields of some of the products of the radiolysis. The rate of energy transfer to the medium by the radiation, namely, the linear energy transfer (L.E.T.), determines the spacial orientation of the spurs. L.E.T. is usually measured in eV./Å and varies with the type of radiation. It is small (~ 0.02 eV/Å) for Co^{60} γ-rays and high energy electrons, medium (~ 0.2 eV/Å) for low energy electrons and β-particles, and large (~ 10 eV/Å) for heavy nuclear particles such as α-particles and Li nuclei. L.E.T. also increases as the energy of the particle decreases down the track. The different chemistry resulting from different L.E.T. radiations

originates from the different separation of the spurs down the track, since intraspur reactions are competing with diffusion of radicals from the spurs. For high L.E.T. tracks the spurs are nearly overlapping so that molecular product formation is dominant, whereas in γ-radiolysis for instance, most radicals completely escape from the spurs.

(iii) Absorbed Dose

In order to get an absolute measure of the yield of any species formed by the radiation, it is necessary to know how much energy is deposited in the medium by the radiation. The amount of energy deposited is usually known as the absorbed dose and has many units, the most common of which is the "rad". One rad is defined to be equivalent to the deposition of 100 ergs gm^{-1} (i.e. 6.24×10^{13} eV. gm^{-1}).[3] There are a variety of methods used to measure dose (dosimetry) and they vary from chemical reactions with known yields to electronic devices capable of estimating the number of particles.[4]

(iv) G-Values

The yield of a species formed or destroyed in a radiation-chemical process is known as the "G-value". It is defined as "the number of molecules, ions, atoms, free radicals, etc. which are formed (or disappear) when the system has absorbed 100 eV. of ionizing radiation energy".[5] G-values are normally in the range of 0-10 for primary processes, although G-values greater than ten may occur for chain reactions.

(c) Radiation Chemistry of Liquid Water[6]

The radiation chemistry of liquid water and aqueous solutions has been the subject of numerous investigations during the past decade. "The process confidently believed to occur upon irradiation of liquid water are the following

$$H_2O \xrightarrow[\text{radiation}]{\text{ionizing}} H_2O^+ + e^- \text{ or } H_2O^* \qquad (1)$$

$$H_2O^+ + H_2O \longrightarrow H_3O^+aq + OH \qquad (2)$$

$$H_2O^* \longrightarrow H + OH \qquad (3)$$

$$e^- \xrightarrow[\text{to solvent}]{\text{energylosses}} e^- \xrightarrow[\text{thermal of } H_2O]{\text{polarization}} e^-aq \qquad (4)$$

$$e^-aq + H_2O \longrightarrow H + OH^-aq \qquad (5)$$

where H_2O^* represents an unspecified excited state.[7] These reactions (2) - (5) represent the physiochemical stage of the radiolysis and lead to the formation of the products of the radiolysis by the chemical stage which consists of reactions such as

$$OH + OH \longrightarrow H_2O_2 \qquad (6)$$

$$H + H \longrightarrow H_2 \qquad (7)$$

$$e^-aq + e^-aq \longrightarrow H_2 + 2OH^-aq \qquad (8)$$

$$H + OH \longrightarrow H_2O \qquad (9)$$

$$H, OH, e^-aq + S \longrightarrow \text{products} \qquad (10)$$

where S represents an unspecified solute present in the system. Reactions (6) - (9) may occur within the spurs to form the

molecular products and reaction (10) occurs after diffusion of the species from the spurs when a solute (S) is present. The yields of the various radicals and products of the radiolysis are dependent upon many factors such as the nature of the radiation (i.e. its L.E.T.) and the nature of the solution. For high energy electron irradiation of pure water at pH7, the following yields are obtained[2]

$G_{e^-aq} = 2.3$ $\quad G_H = 0.6$ $\quad G_{OH} = 2.2$

$G_{H_2O_2} = 0.71$ $\quad G_{H2} = 0.42$ $\quad G_{-H_2O} = 3.6$

The excited water molecules formed in the radiolysis by reaction (1) are generally in an unspecified electronically excited state and they are usually ignored since it is possible to adequately explain the radiolysis of liquid water without including any contribution from excited molecules.[2] The assumption, most often made, is that the excited molecules either return to the ground state by a non-radiative process or else dissociate to H and OH radicals which have little excess energy and they merely recombine causing no net chemical change.

2. Cerenkov Radiation

Cerenkov radiation is a phenomena associated with charged particles moving through a medium at a speed greater than the phase velocity of light in that medium. The phenomena takes the form of electromagnetic radiation emitted by the medium in the visible and ultraviolet regions of the spectrum. It can be considered as analagous to the sonic shock wave produced

by a projectile traveling at greater than the velocity of sound or to the more familiar case of the bow wave of a ship moving through water when its speed is greater than that of the surface waves on the water.

Cerenkov radiation was first observed by Mallet[9] in 1926 but it was not until 1934, when Cerenkov[10] studied the effect, apparently unaware of Mallets' work, that the radiation was characterized. Following Cerenkovs' work in 1934, Frank and Tamm[11] developed the theoretical basis for the radiation in 1937 and this was later modified and expanded.

A simple treatment of the theory of Cerenkov radiation may be given as follows.[12] Assume that as a charged particle travels through a medium, an electromagnetic wave is emitted from each point along the particles' track, due to a polarization of the molecules in the region of the track and then subsequent relaxation of the polarization as the particle passes. These waves will be able to constructively interfere, as shown by the Huygens construction in Fig. 1 if the wavelets from

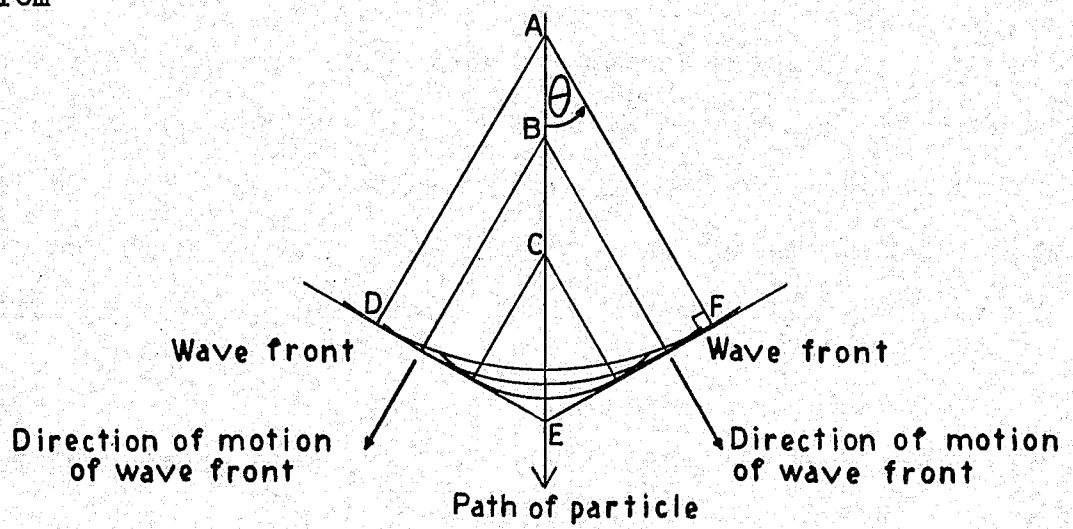

Fig.1

points A,B,C, on the particles' path arrive in phase at the conical wavefront, shown in cross section as DEF. This is possible if, while the light wavefront passes from A to F, the particle passes from A to E. Considering the velocity of the particle to be v, the refractive index of the medium n and the velocity of light in free space C, then the phase velocity of light in the medium is C/n. The condition for constructive interference then follows as

$$\frac{AF}{C/n} = \frac{AE}{v} \qquad \text{i.e. } \frac{AF}{AE} = \frac{1}{\frac{v}{C}\,n} \tag{vii}$$

$$\frac{AF}{AE} = \cos\theta = \frac{1}{\beta n} \tag{viii}$$

where β is the relativistic velocity v/c. Hence the "Cerenkov relation" has been derived.

$$\cos\theta = \frac{1}{\beta n} \tag{ix}$$

It follows that, since cos θ must be $\leqslant 1$, this is only possible if $1/\beta n \leqslant 1$, i.e. if

$$v \geqslant \frac{c}{n} \tag{x}$$

Thus the threshold condition for Cerenkov radiation is that the velocity of the particle must be greater than the phase velocity of light in the medium. Two other properties are evident from relation (ix). There is, for an ultrarelativistic particle ($\beta = 1$), a maximum angle for emission given by

$$\theta_{max} = \cos^{-1}\left(\frac{1}{n}\right) \tag{xi}$$

and furthermore, as the electrons' velocity approaches the other

extreme, namely $\beta = 1/n$, the radiation direction coincides with the particles path. The other property of Cerenkov is that the radiation is in the infra-red, visible and near ultraviolet regions of the spectrum where $n > 1$. Emission in the X-ray region is impossible since $n < 1$ due to dispersion of the medium and equation (ix) cannot be satisfied.

A further property of Cerenkov radiation which comes out of the constructive intereference condition is its polarization. In order that the condition be satisfied, it is necessary to require that the electric vector $\vec{E}$ of the light be everywhere perpendicular to the surface of the Cerenkov cone and the magnetic vector $\vec{H}$ tangential to this surface. Hence the light should be linearly polarized.

The duration of the Cerenkov light emission pulse is, to a first approximation, determined by the velocity of the particle and the length of its track. Hence a pulse duration of the order of 10^{-10} seconds would be observed for a single electron traveling a distance of 3 centimeters.

The radiation yield and spectral distribution of Cerenkov emission can be theoretically determined by a solution of the wave equations and Maxwells' equations for the problem. The original treatment of the problem by Frank and Tamm, as given by Jelley[8], makes the simplifying assumptions that (i) the medium is a continuum and microscopic structure is ignored, (ii) dispersion can be ignored, (iii) the medium is a perfect isotropic dielectric, (iv) the electron can be considered

to move at a constant velocity and (v) the medium is unbounded with the track length infinite. Their solution to the problem gives the result[8]

$$\frac{dW}{dl} = \frac{e^2}{c^2}\int_{\beta n>1}\left(1-\frac{1}{\beta^2 n^2}\right)\omega\, d\omega \qquad \text{(xii)}$$

where W is the total energy radiated by the electron through the surface of a cylinder of length l, whose axis coincides with the line of motion of the electron. ω is the frequency of the radiation, β, the relativistic velocity and n, the refractive index. This integral may be solved by the introduction of the appropriate limits, to give an equation of the form[8]

$$N = 2\pi\alpha\, l\left(\frac{1}{\lambda_2}-\frac{1}{\lambda_1}\right)\left(1-\frac{1}{\beta^2 n^2}\right) \qquad \text{(xiii)}$$

where N is the number of photons, within the spectral range defined by λ_1, and λ_2, emitted by a single electron, l is the track length and α is a fine structure constant equal to 1/137.

The spectral distribution of the radiation may be expresses in several ways, two of which are[8]

$$\frac{d^2N}{dl\,d\lambda} \propto \frac{1}{\lambda^2} \qquad \text{(xiv)}$$

(number of photons per unit path per unit wavelength interval)

$$\frac{d^2W}{dl\,d\lambda} \propto \frac{1}{\lambda^3} \qquad \text{(xv)}$$

(energy per unit path per unit wavelength interval)

Application of these formulae ((ix) - (xv)) to the case of a 500 keV. electron ($\beta = 0.87$), penetrating a depth of 1 millimetre into water, where n = 1.34, shows that $\theta_{max} = 30^\circ$

and the number of photons emitted, between 4000 and 6000 Å, by a single electron is about 10.

A more sophisticated and exact treatment of the theory of Cerenkov radiation, in which the effects of finite track length, slowing down of the particle, dispersion and discontinuity of the medium are included, gives only very slight modification to the formulae derived from the original theory.

3. Previous Investigations of Light Emission from Irradiated Water

At least ten investigations have been made into the phenomena of luminescence of irradiated water. In all but one of these reports, no appreciable light emission other than Cerenkov radiation was noted.

The first investigations of the phenomena were made by Mallet[9] in 1926-1929 and Cerenkov[10] in 1934-1938. Mallet observed the emission from water irradiated with radium γ-rays and made an attempt to determine its spectrum, concluding only that the emission spectrum was continuous. Cerenkov made a more comprehensive study of the light and determined its spectrum, angular distribution and intensity. Since known quenching agents had little effect on the intensity of the emission, he concluded that the light emission was not due to normal de-excitation processes. By observing the influence of a magnetic field on the radiation, he also showed that the emission was due to the secondary electrons produced in the

medium by the γ-rays.

In the period following Cerenkovs' work, seven more papers[13-19] were published which supported the original discovery. The authors used a variety of techniques, including spectrographs and photomultipliers, to determine the emission spectra and photon yields from the irradiations of water with a variety of radiation sources, direct current electron accelerators, γ-rays, β-rays and α-particles.

In 1963, Sitharamarao and Duncan[20], studied the light emission from Co^{60} γ-irradiated water, using sensitive cadmium sulfide crystal detector. They report observing four broad bands in the visible and ultraviolet region of the spectrum and also the characteristic Cerenkov radiation produced by the Compton electrons. They assigned the bands, on the basis of little evidence, to various processes of the radiolysis.

In 1966, Czapski and Katakis[21], reinvestigated the system, using as a radiation source the β-particle from tritium in the form of T_2O. The maximum energy of this β-particle is below the threshold energy for Cerenkov radiation. They report observing an extremely low intensity light emission with a photon yield $G_{h\nu} \leqslant 10^{-5}$, which is at least four orders of magnitude less than that reported by Sitharamarao and Duncan. They were unable to measure the spectrum accurately due to the low intensity of the emission and they did not make any assignment as to its origin.

4. Scope of the Present Investigation

Partly in view of the apparent conflict between the two most recent investigations, it was decided to reinvestigate the system using as a radiation source an intense pulse of high energy electrons. This source had the following advantages over radiation sources used previously for similar investigations: (i) it was pulsed and consequently emission lifetime measurements would be possible, (ii) the radiation intensity during the pulse was higher than other sources by a factor of 10^6 (Sitharamarao and Duncan, who reported observing emission, were using a radiation intensity several orders of magnitude larger than that used by Czapski and Katakis), (iii) the electron energy could be varied from 0.5 MeV. to below the Cerenkov threshold and (iv) the high energy electrons responsible for Cerenkov radiation were unidirectional and thus the isotropy (and possibly the polarization) of the light emission could be studied. The aim of the investigation was therefore to determine if there was any light emission, other than the expected Cerenkov radiation, and if so, to determine its emission lifetime, spectrum, yield and origin.

A consideration of the events occuring in the system during and after the radiation pulse leads to some predictions as to the nature of the light emission that one might expect to see.

When a thermalized electron, formed in the ionization process, becomes hydrated, to form the hydrated electron [22],

it must lose about 2 eV. of energy since the average trap depth is believed to be 2-3 eV. Since this process occurs in a time of the order of 10^{-11} seconds[2], the dielectric relaxation time of water, the energy might well be liberated in the form of photon emission and thereby give an emission spectrum for the formation of the hydrated electron complementary to its already well established absorption spectrum.

Another possible source of light emission might be from excited water molecules. Although the first singlet excited state of water is a dissociative level, a theoretical prediction of a low lying triplet energy level has been made[23]. Since the ionization potential of water is about 12 eV. and for every 100 eV of energy deposited in the system only about 3 ion pairs are formed, it follows that more than half of the energy deposited in the medium is used in excitation of water molecules apparently with no resulting chemical change. Hence a possible source of light emission is from triplet excited water molecules.

Other possible sources of light emission are excited OH radicals, which are known to emit in the near ultraviolet in the gas phase[24], and possibly radical-radical reactions of the type

$$R_1^* + R_2 \longrightarrow R_3^* + R_4 \qquad (11)$$

$$R_3^* \longrightarrow R_3 + h\nu \qquad (12)$$

where R_1^* and R_3^* represent an unspecified electronically

excited radical or molecule.

Indeed one might speculate that, because of the apparent very inefficient use of energy in the radiation chemistry of water, it would be surprising if none was utilized in photon emission.

EXPERIMENTAL

1. Electron Accelerator

A Febetron pulsed electron accelerator, shown in Fig. 2, manufactured by Field Emission Corporation, McMinnville Oregon, was used as the radiation source for this investigation.

The accelerator, model 701-2660 pulser with model 5235 electron tube, produced an extremely intense pulse of 0.52 MeV. electrons. The peak beam current, at the tube window, was about 1000 amperes and the beam pulse shape, shown in Fig. 3(a), was roughly triangular with a half width of about 20 nanoseconds. Both the pulse shape and peak beam current were extremely reproducible from pulse to pulse with a root mean square variation of about $\pm 3\%$. The energy of the output beam electrons was variable from near zero to 0.52 MeV and it depended on the D.C. charging conditions of the pulser, which operated on the Marx Surge Circuit principle. The corresponding beam current also varied with charging voltage since the impedance of the tube was nearly constant. The maximum radiation dose available was of the order of 10^6 rads, with the corresponding dose rate of about 10^{13} rads/sec averaged over the pulse.

A mounting flange on the accelerator allowed the irradiation cell to be positioned at a distance of about 4 centimeters from the electron tube window.

2. Electron Beam Current Measurements

The electron beam current was measured using an apertured Faraday cup. The Faraday cup and aperture are shown in Fig. 4. It consisted of two concentric aluminum cylinders, open at one end, coupled across a T & M Research Products model GR-1-05 current viewing resistor which had an impedance of 0.0507 ohms. The output of the resistor was coupled to a length of doubly shielded RG 58/U coaxial cable which terminated in 50 ohms at the vertical input of the model 82 plug-in amplifier of a Tektronix model 585A oscilloscope on which the voltage pulse developed across the current viewing resistor was displayed. The aperture was an aluminum cylinder machined so that the Faraday cup could be placed in an equivalent position to the irradiation cell on the accelerator. In this way the apertured Faraday cup measured the beam current transmitted into the irradiation cell and gave an estimate of the radiation dose. The appropriate electron window material used in the cell was also included on the aperture to take into account back scattering and attenuation of the beam by it. The sensitivity of the resistor was about 20 amps/volt and the voltage range of the amplifier was 0.002 V. to 400 V. so that currents in the range from 0.04 to 8000 amperes were measurable with this technique.

The electron beam current-time pulse shape was monitored on the oscilloscope by scanning the time base at the appropriate

sweepspeed and photographing the oscilloscope traces using a Polaroid camera and high speed film. The typical pulse shape is shown in Fig. 3(a). The peak beam current measured for an 0.002 inch stainless steel electron window and full charging voltage was typically 170 ± 5 amperes and was reproducible, from pulse to pulse, to within 5%. The variation of beam current with charging voltage was determined by this technique and the results are shown in Fig. 5. The cutoff of current at 12 KV. charging was the result of complete absorption of the electrons by the stainless steel electron window on the aperture and the titanium window of the electron tube.

Integration of the current-time pulses gave the total number of electrons per pulse. Typical results were, for 170 ampere peak current at full charging voltage, $2.0 \pm 01 \times 10^{13}$ electrons per pulse.

3. Dosimetry

The absorbed radiation dose, or total amount of energy deposited in the irradiation cell, was determined approximately by use of a calorimetric technique. An aluminum disk of appropriate diameter and of sufficient thickness to stop all of the electrons ($\sim$ 0.032 inch) was placed in a position equivalent to the sample in the irradiation cell and thermally insulated from the surroundings. A chromel-alumel thermocouple junction was attached to the disk and the temperature rise upon irradiation of the disk with a single pulse was determined by measuring

the change in potential of the thermocouple junction with a microvoltmeter. Knowing the weight of the aluminum disk, its specific heat and the temperature change (calculated from the change in potential of the junction and its known sensitivity[25]) the total energy deposited in the disk could be calculated. The uncertainty in the value obtained in this manner is primarily due to back scatter of the electrons from the aluminum disk and uncertainty in the calibration of the voltmeter. These combined errors are estimated to be less than 20%. Typical results for full charging potential and 0.002" stainless steel window material in the cell were, $0.85 \pm 0.17 \times 10^{19}$ eV. per pulse. (This value is confirmed by calorimetric and chemical dosimetry done by D.A. Head[26] on the same accelerator).

Other methods of dosimetry available were: (1) calculation of the energy deposited by combining the total number of electrons, as measured with the Faraday cup, with the average electron energy, estimated from a consideration of the mean energy losses in the thin stainless steel cell window. (Using the calorimetric value of total energy and the Faraday cup measurements, the average electron energy was calculated to be $0.42 \pm 0.08 \times 10^{6}$ V., which seemed reasonable) (2) chemical dosimetry, such as the hydrogen yield from irradiated cyclohexane or (3) measuring the optical density change induced in a dyed cellophane and obtaining the dose from a calibration curve.[27]

4. Spectral Analysis Systems

(a) Photomultiplier-Interference Filter Wedge Spectrometer

A photomultiplier-interference filter wedge spectrometer was designed so that the emission lifetime and the spectral characteristics of the light emission could be determined simultaneously. The spectrometer is shown in Fig. 6 (a) and 6 (b). Fig. 6 (a) is a photograph of the spectrometer and Fig. 6 (b) is a plan view of it showing its mode of operation. The interference filter wedge used was a VERIL S 200 continuous line filter and the photomultiplier was an R.C.A. Victor 1P28.

Variation of the position of the wedge filter with respect to the slits was accomplished with the aid of the control rod, which was marked with small divisions so that the exact position of the filter was known. This variation changed the band of wavelengths seen by the photomultiplier and by successively scanning the whole filter a complete spectrum could be obtained from 4000 to 7000 Å . The dispersion of the filter was about 25 Å per millimeter.

Light emitted from the irradiation cell was directed at the spectrometer by means of a front silvered plane mirror and two cylindrical light collimators as shown in Fig. 7. The short initial collimator was nickel plated on the inner surface so that the maximum amount of light possible was collected. The second collimator, at right angles to the first, was painted flat black so that only a roughly parallel beam

of light reached the slits of the spectrometer. The collimators and the spectrometer were enclosed in lead boxes, as shown in Fig. 7, in order to eliminate X-ray effects on the photomultiplier and also to attenuate the primary X-ray beam of accelerator.

The photomultiplier load resistance had to be 50 ohms in order to match impedance with the coaxial cable and avoid the use of a cathode follower. (The interdynode capacitance of the photomultiplier limits the size of the load resistance to less than 500 ohms if 100 MHz. frequency response is required). The RG58/U coaxial cable leading from the photomultiplier to the oscilloscope was doubly shielded and connected to the input of the vertical amplifier of the Tektronix 585A oscilloscope. The anode current pulse, developed across the photomultiplier load resistance, was then displayed on the oscilloscope as a negative voltage pulse and it was photographed with a Polaroid camera. The maximum anode current permissible, before saturation effects[28] caused non-linearity of response of the photomultiplier, was about 2 milliamperes, which corresponded to a maximum voltage pulse across the 50 ohm load of 100 mV.. Since the maximum sensitivity of the oscilloscope amplifier was 10 mV./cm., only a very limited range of light intensity was measurable. However, by interposition of neutral density filters in the light beam, the effective intensity range could be expanded considerably. Further amplification of the small voltage pulses by means of an auxilary amplifier

was not possible because of the high frequency involved.

It was also necessary, when operating the photomultiplier with large anode currents, to provide a large dynode resistor chain current in order to prevent non-linearities due to fluctuations of the dynode voltages during the pulse. As a result, the 1P28 was operated at 500 V. and 10mA.D.C.. (Note: The photomultiplier could not be operated satisfactorily at larger voltages (and thus higher sensitivity) due to a large random noise level caused by the small load resistance.) A Fluke stabilized D.C. power supply was used to maintain these conditions.

Wavelength calibration of the detection system was obtained by use of a mercury vapour lamp and a He-Ne laser. The anode current of the photomultiplier was measured as a function of the position of the wedge control rod for both light sources, using a small slit opening. The He-Ne laser was used as a wavelength marker and the mercury emission lines were used to check the linearity of the dispersion of the filter wedge. The device was found to be linear over the range 4000 to 7000 Å .

Calibration of the spectral sensitivity of the system was performed with the use of a calibrated quartz-iodine lamp placed at an equivalent position to the irradiation cell. The anode current was again measured as a function of the position of the wedge control rod. From a knowledge of the wavelength calibration of the control rod and the emission

spectrum of the calibrated lamp, the spectral sensitivity of the detection system was obtained. It is shown in Fig. 8.

The procedure for determining an unknown emission spectrum with the spectrometer was as follows. The sample was irradiated in the cell, which was positioned in front of the light collimator, and the anode current pulse of the photomultiplier was measured using the oscilloscope. This was repeated for each position of the control rod, using a single pulse and fresh sample of liquid for each wavelength band. The peak anode current, which was proportional to the intensity of the light, was then corrected for the variable spectral sensitivity of the detection system and the relative emission spectrum was thus obtained. It was not possible to determine an absolute emission yield with this arrangement because of difficulties in estimating the fraction of the total light emitted that reached the photomultiplier.

From the shape of the anode current pulses, the lifetime of the emission could be determined if it was longer than 10^{-8} seconds. Lifetimes shorter than this were not measureable since the fall time of the electron pulse was 10^{-8} seconds.

The pulse to pulse reproducibility of the anode current pulses of the photomultiplier for identical operating conditions of the spectrometer was very good. A variation of the order of $\pm$ 5% was observed and this was likely due to the

variations in the output electron pulse of the accelerator.

(b) Grating Spectrograph

A large aperture, low resolution, grating spectrograph was also used to determine the emission spectra. This spectrograph is shown in Fig. 9. It was constructed following the design of Bass and Kessler[29] and consisted of a slit and lens arrangement to collect the incident light and focus it on a Bausch and Lomb grating, ruled with 600 lines per millimeter, and a Konica F.P. 35 mm. camera with a 1.4 wide angle lens to record the spectra. Wavelength calibration was performed by use of a mercury vapour lamp and the absolute spectral sensitivity of the system was determined using the calibrated quartz-iodine lamp. The spectrograph was found to be linear in dispersion over the range from 4000 to 6500 Å with a dispersion of about 150 Å /mm. when using a second order diffraction angle.

The film used to record the emission spectra was the fine grained, high speed, panchromatic Ilford HP4. It was developed in fresh Acufine developer for 5 minutes at 72 F. in a spiral tank with gentle agitation, washed for 30 seconds in water, and fixed for 5 minutes in Kodac Rapid Fixer and Hardener.

The emission spectra of the irradiated liquids and the plastic scintillator were determined by positioning the irradiation cell in front of the slits and irradiating the sample with a sufficient number of pulses to give a measureable

density on the film. The film was protected from the primary X-ray beam with a sheet of lead between the camera and the accelerator. Wavelengths were marked on the film by exposing the centre portion of the film to a mercury vapour lamp.

The true emission spectrum was then obtained by the following procedure which corrects for the non-uniform spectral response and the non-linear exposure-density relationship for the film. A series of exposures for the standard quartz-iodine lamp at various exposure times were made and from the densitometer tracings of the films, the characteristic curves, showing exposure versus density, were plotted for various wavelengths. The unknown spectrum was then measured on the densitometer and the appropriate relative exposure was determined from the characteristic curves. This relative exposure was then corrected for the spectral distribution of the quartz-iodine lamp and the emission spectrum of the sample obtained. The spectral sensitivity of the spectrograph was determined in a similar manner and it is shown in Fig. 10.

An estimate of the total emitted photon yield from irradiated water was evaluated by comparing the wavelength integrated densities for the water emission and the standard lamp in equivalent positions and relating the relative densities to a relative number of photons in the spectral region involved. Taking into account the geometries involved and knowing the absolute intensity of the quartz-iodine lamp, an estimate of the number of photons emitted by the water was found and

this converted to a G-value using the known radiation dose.

5. Densitometry

A Joyce double beam, recording microdensitometer was used to measure the density of the films from the spectrograph and the 180° camera. This instrument measured the density of the film, relative to the background, directly in density units and laterally scanned the film at the same time, recording the density on chart paper. The density calibration of the instrument was checked by use of neutral density filters and it was found to be linear over the density range from 0 to 1.6.

6. 180° Camera

A 180° camera was designed and constructed to enable measurement of the angular distribution of the light emission. Shown in Fig. 11, it consisted of a hemicyclindrical piece of plexiglass enclosed on the other three sides by a rectangular box with a collimated entry port (a 1/8" hole in a large aluminum cylinder) for the electron beam at the centre of the half cylinder. The inner surface of the collimator was covered with a thin piece of aluminum foil so that the vessel was water tight and a filling port was included so that solutions could be changed. Provision was made for attaching a photographic film to the curved surface of the cylindrical window. The curved surface was painted flat black on the inside along its edges, leaving a clear 1" wide band around the centre. In this way, a background measurement of the light contribution from Cerenkov

radiation from the plexiglass itself and the X-ray effects on the film were determined. (The action of the X-ray beam on the plexiglass generated sufficient light to partially darken the film). The remainder of the box portion of the camera was also painted flat black on both surfaces in order to reduce the effects of scattered and stray light.

The film, Ilford HP4, was exposed to the light generated by several pulses and then developed. A densitometer trace of the centre portion of the film and an adjacent portion then gave, by difference, the angular dependence of the light emission. The angular dependence was determined for water, a plastic scintillator and a high purity quartz glass.

7. Irradiation Cell and Water Flow System

Some preliminary experiments were performed using an irradiation cell made from aluminum and an electron window of aluminum foil. However, this cell was found to corrode, with the formation of white deposits of aluminum hydroxide, on prolonged contact with water. Stainless steel was then tried as a cell and window material and it was found to be satisfactory with no visible corrosion even after 48 hours of contact with water.

The stainless steel cell is shown in Fig. 12. It consisted of a ring of stainless steel, appropriately machined, with a high purity quartz optical window cemented on one side and provision for a thin stainless steel foil electron window

on the other side. The electron window was held in place by a teflon ring on the cell and a rubber "O" ring on the aluminum mounting flange. The cell also had filling and draining ports, with Kovar glass-metal seals, to allow solutions to be flowed through it.

The water flow system consisted of a two litre flask fitted with a fritted glass bubbler, (to allow degassing of the solution by the passage of helium through it), a pressure release valve and a glass connecting line to the irradiation cell. The connecting line was attached to the entrance port of the cell by means of a ball and socket joint. After degassing the solution, by bubbling helium through it for at least a half hour, the flask was pressurised and the water forced into the cell. The flow through the cell was regulated by means of a stopcock on the exit port of the cell. The solution, in the cell, was generally changed after each pulse by opening the stopcock and allowing the solution to flow through the cell for a few seconds. This was done so that impurities formed by the radiation would not build up in the solution.

8. Actinometry

An attempt was made to estimate the total number of photons emitted by the sample using a chemical actinometer. Potassium ferrioxylate solutions were used following the method of Parker[30,31]. It was found that no change in optical density of the developed solutions could be detected following expo-

sure of the actinometer to the light emission from either water or a plastic scintillator.

9. Spectrofluorimetry

The emission spectrum of the plastic scintillator was obtained with an Aminco-Bowman Spectrophotofluorometer. This was done so that a check could be made on the calibration of the light detection instruments used in this investigation. The spectra obtained from the grating spectrograph and the interference wedge spectrometer for the plastic scintillator were compared with that obtained from the spectrofluorometer. All three spectra were found to be very similar.

10. Materials

(a) Water

Doubly distilled water was used in all experiments. The second distillation was made from acidic permanganate solution.

(b) Scintillator

The plastic scintillator, NE 102, manufactured by Nuclear Enterprises Ltd., was used as a check of the calibration of the spectrograph and the spectrometer. The scintillator was in the form of a thin plastic sheet and it was cut into circular disks which fit inside the irradiation cell.

(c) Photographic Materials

Acufine developer and Kodac Rapid Fixer and Hardener were used. The solutions were made using distilled water.

(d) Other Materials

Analytical grade KOH and H_2SO_4 were used to prepare acidic and basic solutions. The Benzene, Methanol and Cyclohexane were reagent grade and the compressed gases, He and O_2, were regular commercial grade.

11. Electrical Noise

Due to the intense electrical and magnetic fields generated by the Febetron pulser and the electron beam, it was necessary to install a good high frequency grounding system connected to all the electronic equipment in use. It was also necessary to filter the 110 V. input power lines to the oscilloscope and photomultiplier power supply with a radiofrequency line filter. All coaxial cables used were doubly shielded using copper braid surrounded by thick copper pipe. The resulting noise level on the oscilloscope traces was less than 5 mV..

RESULTS AND DISCUSSIONS

1. Preliminary Investigations

A few preliminary observations of the light emission from water irradiated with a pulse of electrons gave an indication of its general characteristics.

Visual observation of the emission, by reflecting the light beam with a mirror to an observer behind the radiation shields, indicated that the light emission was short lived (lifetime less than several seconds) and that it had a bluish-white spectral character.

An attempt was made to obtain a low resolution spectrum using interference filter wedge and a photographic film. A plexiglass rod light guide was used to transmit the light beam from the irradiation cell to the slits in front of the interference wedge. (The wedge and film could not be placed directly in front of the cell because the X-ray beam from the accelerator caused appreciable darkening of the film.) This experiment failed to obtain a spectrum since a blank run, where the light from the cell was prevented from entering the light guide, revealed that a considerable portion of the darkening of the film was due to light produced in the light guide itself. This light was probably Cerenkov radiation from the plexiglass produced by the X-ray beam generated as Bremsstrahlung when the electrons were stopped in the water and the electron tube window. Similar experiments which involved using a photo-

multiplier tube instead of the photographic film were also invalidated by the balnk run.

Since visual observations confirmed the presence of light emission from the water, a more elaborate experimental setup was designed and constructed so that an accurate assesment of the emission could be made. The results of the experiments performed with this apparatus are recorded in the following sections.

2. The Angular Dependence of the Light Emission

In Fig. 13 the angular dependence of the light emission from water, quartz glass and a plastic scintillator is shown. This data was obtained from measurements of the density of films from the 180° camera as a function of angle using the densitometer. The graphs show the density difference, ΔD, (between the portion of the film exposed to the light emission and the adjacent background density) at a given angle θ plotted as a function θ, where θ is the angle between the direction of motion of the elecgron beam and the emitted light beam.

In the case of the plastic scintillator, the sample was a hemicylindrical piece of polished plastic which was fixed over the entrance port for the electrons in the 180° camera whereas for quartz an optical window was used. In both cases the camera was filled with water to reduce the X-ray effect on the film and diminish reflection and refraction of the light.

As can be seen from the curves on Fig. 13, water appears

to emit light preferentially in the forward direction whereas the scintillator shows an emission which is isotropic, as would be expected for fluorescence.

The experiment with quartz was performed in the hope that high purity quartz would show only a Cerenkov radiation emission and thereby be a valuable comparison for the water experiment. However it appears that the emission from quartz has an angular dependence unlike that expected for just Cerenkov radiation. Kawabata and Okabe[32] have observed a long lived luminescence in irradiated quartz, which, coupled with the expected Cerenkov radiation, might account for the angular dependence found in this work.

The relative magnitude of ΔD for the water, quartz and scintillator have little significance because the background densities were not the same. Furthermore, in the water and quartz experiments, several pulses were needed to give sufficient exposures.

From these experiments it is evident that the luminescence from water has an angular distribution different from normal fluorescence. The experimentally observed angular dependence is, however, in reasonable accord with it being almost entirely Cerenkov radiation. For water, the maximum angle for Cerenkov radiation for 0.52 MeV. electrons is $\theta_{max}=30^{\circ}$ and as the electrons slow down the angle of emission becomes smaller. But, in addition, elastic scattering of the high energy electrons will cause a broadening of the angular distribution. A complete analysis of the expected Cerenkov distribution is impossible

without a detailed knowledge of the primary interaction processes of 0.52 MeV. electrons. These two effects might indeed give rise to a distribution similar to the observed one.

3. Variation of the Emission Intensity with Electron Energy

The intensity of the light emission from water and from the plastic scintillator was measured as a function of the energy of the incident electrons using the interference filter wedge spectrometer. The energy of the electrons was varied by varying the charging voltage of the accelerator.

The results of this investigation are shown in Fig. 14 where the peak light intensity (in arbitrary units) is plotted as a function of the charging voltage of the accelerator. The corresponding maximum energy of the incident electrons (data supplied by Field Emission Corporation and corrected for energy loss in the stainless steel window) is also shown on the ordinate. The curves are normalized to the same intensity at 27.5 KV. charging voltage, but in actual fact the scintillator intensity was considerably greater than that of water. The data was obtained for a narrow wavelength band centred at 5060 Å.

As can be seen by comparing the curve of Fig. 14 for the scintillator with the curve of beam current as a function of charging voltage given in Fig. 5, the scintillator emission intensity and beam current have a similar dependence on charging voltage. Water, on the other hand, appears to show a more complex behaviour, with an apparent cutoff of emission intensity

at about 240 KV electron energy. These features of the emissions are shown more clearly if one plots the peak light intensity divided by the product of the electron energy and peak beam current (i.e. something which is proportional to a G value for photon emission) as a function of electron energy. This is shown in Fig. 15. It is evident from this graph that the emission yield for water increases as the electron energy increases and also has a zero value at electron energies of about 240 KV. In contrast, the emission yield for the scintillator decreases quite rapidly and then levels off as the electron energy increases. The radiation yield for an excitation energy transfer process, such as one might envisage being responsible for fluorescence of the scintillator, should be independent of the electron energy. However, since one is dealing here with extremely high radiation intensities, second order deactivation processes may be the cause of the observed decrease in photon yield.

These results are consistent with the angular dependence results in that they tend to support the view that the emission from water is mainly Cerenkov radiation. The low-energy cut-off of the photon yield at 240 KV is in agreement with the expected value of 260 KV for Cerenkov radiation in water (i.e. when $\beta = \frac{1}{n}$) and the increase in photon yield with increase in electron energy is also as predicted for Cerenkov radiation. In their theoretical treatment of Cerenkov radiation, Frank and Tamm[11], establish the relationship

$$N = 2\pi\alpha l\left(\frac{1}{\lambda_2}-\frac{1}{\lambda_1}\right)\left(1-\frac{1}{\beta^2 n^2}\right) \qquad \text{(xii)}$$

where N is the number of photons emitted in spectral range between λ_1 and λ_2 by a single electron, α is a fine structure constant equal to 1/137, l is the distance the electron travels while it is radiating, β is the relativistic velocity and n is the refractive index. Thus for a given spectral range, there should be a linear relationship between N and $l \cdot (1-1/\beta^2 n^2)$. Fig. 16 shows the peak light intenisty for water at 5060 Å divided by the peak beam current (i.e. something proportional to the number of photons per incident high energy electron) as a function of $l\cdot(1-1/\beta^2 n^2)$. l was calculated from the difference in energy between the energy of the incident electron and the energy of the Cerenkov cutoff and using the linear energy transfer value for the high energy electron in water. β was calculated from the electron energy taking into accoount its relativistic mass. The linearity of this plot may be interpreted as either a corroboration of the notion that the light observed is Cerenkov radiation or as experimental verification of the theory of Frank and Tamm.

4. The Emission Lifetime

Typical photomultiplier anode current pulses for the light emission from irradiated water and scintillator are shown in Figs. 3(b) and 3(c) respectively. These figures are copies of the photographs taken of the actual oscilloscope traces. Comparison of Figs. 3(b) and 3(c) with 3(a), the time

dependence of the electron pulse, indicates that the emission lifetime from water is $\lesssim 10^{-8}$ seconds and from the scintillator $\sim 10^{-8}$ seconds. The exact shape of the water emission is also noteworthy, in that the secondary peak which is present in the current pulse, is absent or very small in the light emission in comparison to the main peak. Both of these observations can be explained on the basis of Cerenkov radiation. The lifetime of Cerenkov radiation is determined, to a first approximation, by the time required to stop the electrons and it is therefore of the order of 10^{-11} seconds. This is to be compared with fluorescence lifetimes which may be 10^{-9} seconds or longer. Secondly, if the energy of the electrons in the secondary peak is substantially less than that of the primary peak, as seems likely because its intensity has a much stronger dependence on changing voltage than the primary peak, then for Cerenkov radiation (but not for fluorescence) the intensity of the light emitted by these electrons (per electron) would be expected to be very much less than that emitted by the primary electrons.

5. Actinometry

The failure of the actinometer to measure any light emission from the water is not surprising if one is dealing only with Cerenkov radiation. Since a pulse contains only about 2×10^{13} electrons and the theory of Frank and Tamm predicts only about 10 photons per 0.52 MeV electron in the range of 3000 - 5000 Å (the strong absorption band of the ferrioxylate

actinometer) more than 50 pulses would have been required to exceed the limit of detection of this actinometer as given by Parker[30,31]. The failure of the actinometer to register a change with the scintillator is however surprising. Perhaps there is an important intensity effect due to second -order processes under the enormous light intensities ($\sim 10^{22}$ photons/ cm.^{2}/sec.) involved in this experiment.

6. The Emission Spectrum

(a) Photomultiplier - Interference Filter Wedge Spectrometer

The emission spectrum of pulse irradiated water as determined on the photomultiplier - interference filter wedge spectrometer is shown in Fig. 17. This graph is a plot of the relative number of photons emitted in a given wavelength band as a function of wavelength. The data was obtained from the peak of the anode voltage pulses measured for various positions across the interference filter wedge and corrected for the spectral response of the entire optical arrangement and detection apparatus. The uncertainty in the relative number of photons, shown by the appropriate error bars, is almost entirely due to the uncertainty in the calibration of the spectral response of the spectrometer. The dotted line is a plot of c/λ^2 versus λ (where c is an arbitrary constant chosen so that a large portion of the experimental points fall on the line) and represents the expected relative variation of Cerenkov radiation intensity as a function of wavelength.

It appears from Fig. 17 that the observed emission between 4500 -6500 Å is consistent with it being Cerenkov radiation. The deviation of the emission spectrum from the c/λ^2 curve at short wavelength (4000 - 4500 Å) may be due to one of the following reasons: (i) it may be a true emission with intensity greater than Cerenkov radiation; (ii) the interference filter may have been transmitting higher order, lower wavelength light at these wavelengths (i.e. 3rd order 2666 Å at 4000 Å since the filter is second order in interference); or (iii) the calibration of the spectral response of the instrument had a large error at these wavelengths.

Point (iii) can be checked experimentally. If there was a large error in the calibration in this region, then the apparatus would not be able to reproduce a known emission spectrum. The calibration was checked by observing the emission spectrum of the scintillator and treating the data in the same manner as for water. The resulting spectrum is shown in Fig. 18 along with the emission spectrum obtained using the spectrophotofluorometer. Both spectra show the same general shape and exactly the same wavelength of maximum emission. Since the scintillator emission has its maximum in the suspect region, the calibration of the instrument must be at least as accurate as estimated, otherwise the interference filter wedge spectrometer data for the scintillator would have also deviated from the expected values.

Regarding point (ii), if the filter was transmitting

ultraviolet light in the region from 4000 to 4500 Å by a higher order interference, the deviation of the spectrum could be explained, since the yield for Cerenkov radiation in the ultraviolet is much greater than in the visible region. However, according to the manufacturers specifications, the interference filter was cemented to a progressively coloured glass to eliminate higher order transmissions. Since the region of 4000 - 4500 Å occurs at the very end of the filter, it may not have been properly compensated, but this is very unlikely.

It appears that the most likely explanation of the deviation is that it is due to a true emission. Whether this emission results from a "chemical" radiative process, such as fluorescence, or a physical process, such as transition radiation, cannot be decided without further study, although as will be indicated later the same deviation is found for benzene, methanol and cyclohexane, which suggests that it is not "chemical" in nature.

The most significant fact about the general appearance of the spectrum is the c/λ^2 variation which it follows from 4500 - 6500 Å , in agreement with that expected from Cerenkov radiation. (Note: The spectrum between 6500 - 7000 Å could not be determined with this instrument because of the insensitivity of the photomultiplier in this region.)

(b) Grating Spectrograph

The emission spectrum was also obtained using the grating spectrograph in order to determine if there was any long lived,

low intensity emission which would be detectable by a film but not by the photomultiplier technique. The emission spectrum of water was determined by correcting the measured density on the film from the spectrograph for the non-uniform spectral response of the film. The resultant spectrum, plotted as relative number of photons (in arbitrary units) versus wavelength, is shown in Fig. 19. Because of the relative insensitivity of the film to low energy light, the spectrum extends only to 6000 Å . The dotted line is again a c/λ^2 versus λ curve. Uncertainties in the slopes of the characteristic curves used in the data treatment procedure are the main sources of error. These uncertainties are fairly large due to the fact that the data for the characteristic curves was not obtained using the same piece of film as was used to record the water emission. Although identical development procedures were used for both films, the background densities were not the same due to the exposure of the film, in the water experiments, to the X-ray beam. (The slope of the characteristic curve is dependent on the development time.[33])

As can be seen from Fig. 19, the spectrum obtained for water by this technique, has the same features as the spectrum obtained with the spectrometer (shown in Fig. 17). Indeed even the deviation at short wavelengths is present. Since the spectrum was obtained using a second order diffraction angle, the possibility of higher order diffraction occurs here also. However, since the light had to pass through two glass

lenses all of the ultraviolet portion of the light would have been absorbed in the lenses. The possibility of mis-calibration of the instrument in this region is again ruled out on the grounds that the emission spectrum of the scintillator was found to be very similar to the spectra obtained by the other two methods. (The only difference in the spectra was an emission band in the region of 5900 - 6400 Å which was attributed to a phosphorescence emission which the other two methods would not detect.) Hence it appears that the deviation from c/λ^2 at short wavelengths must again be attributed to a true emission.

7. The Effect of Additives

The effect of the addition of impurities on the water emission spectrum was investigated using the grating spectrograph.

It was found that the impurities formed by the radiation had no effect on the emission spectrum of water. (H_2,O_2 and H_2O_2 are formed by the radiation pulse in the water.) In fact, the density-wavelength band on the film for an exposure to the light emission from ten radiation pulses, where fresh water was used for each pulse, was exactly identical to that for an exposure to ten pulses where the same sample of water was used for all ten pulses.

It was also found that the addition of 0.IN. KOH, 0.IN. H_2SO_4 or $\sim 10^{-3}$ M. oxygen had rather little effect on either

the emission intensity or the spectrum. Actually the KOH had no effect on either the spectrum or intensity, whereas H_2SO_4 and oxygen increased the emission yield slightly but the spectral distribution remained unchanged. The increase in the case of H_2SO_4 was about 10% while for oxygen only about 2% change was noted.

These results indicate that (i) radicals or ions which are reactive towards these additives are not involved in the emission process. The addition of acid would convert all of the hydrated electrons to hydrogen atoms by reaction (11),

$$e^-aq + H^+ \longrightarrow H \qquad (11)$$

while the addition of base would convert all of the hydrogen atoms to hydrated electrons by reaction (12).

$$H + OH^- \longrightarrow e^-aq \qquad (12)$$

The presence of hydrogen, oxygen and hydrogen peroxide would also affect the processes occuring by reactions such as (13) - (16).

$$O_2 + H \longrightarrow HO_2 \qquad (13)$$

$$O_2 + e^-aq \longrightarrow O_2^- \qquad (14)$$

$$H_2O_2 + OH \longrightarrow H_2O + HO_2 \qquad (15)$$

$$H_2 + OH \longrightarrow H_2O + H \qquad (16)$$

(ii) There are no normal radiative de-excitation processes from electronically excited water molecules that oxygen at 10^{-3} M. can quench. And (iii) the emission does not result from oxygen itself, or some reaction involving oxygen. De-aeration by bubbling with helium would not completely remove the atmospheric oxygen from the solutions and thus it might

have been contributing to the emission; but since a probable 10^3 fold increase in oxygen concentration did not affect the photon yield such processes can apparently be ignored.

On the other hand, these results are in complete agreement with the emission being composed almost entirely of Cerenkov radiation, since the intensity and spectrum of Cerenkov radiation depends only on the physical nature of the medium (i.e. its refractive index). The slight increase in photon yield for the acidic solution might be accounted for by a difference in refractive index between pure water and 0.1N. H_2SO_4. However, since the absolute difference between the two refractive indices is only about 1%, which would thereby increase the yield by about 2%, a more likely source of the difference is experimental error which is estimated to be of the order of 10%. (The pulse to pulse reproducibility of the accelerator was about 3% and since the results were obtained for a multiple pulse experiment, an error as large as 10% would not be inconceivable.)

8. Comparison of Water with Other Liquids

In order to check the early indication that water appeared to have no emission other than Cerenkov radiation (neglecting for the moment the possibility of some emission in the region of 4000 - 4500 Å) the emission spectra of several other liquids were investigated using the grating spectrograph. A series of experiments were carried out in which the irradiation cell

and the spectrograph were positioned in identical locations and the experimental conditions were the same for all of the liquids. An equal number of pulses was given to each sample and the spectra were recorded on the same piece of film so that a detailed comparison of them could be made. The liquids chosen for the comparison were water, methanol cyclohexane and benzene. These were chosen on account of their differences in structure, sensitivity to ionizing radiations and refractive index.

The results are shown in Fig. 20, where the densitometer tracings of the four spectra are reproduced. It is evident that: (i) water and methanol show identical emission bands, both in absolute intensity and spectrum. (ii) Cyclohexane and benzene gave emission bands which were of greater intensity but identical in shape to the water. (The apparent difference in the shape of the emission bands for water and benzene at the red end of the spectrum is due to the fact that the log (exposure)-density relation for a film is not linear in the region of small densities and in particular a very small change in exposure can give a comparatively large density change. When water was irradiated with more pulses than the benzene, a spectrum of equal density to the benzene spectrum was obtained for all wavelengths). (iii) The order of increasing density of the bands at any given wavelength was water = methanol < cyclohexane < benzene.

These results can only sensibly be interpreted on the

basis that the emission in all four cases is almost entirely Cerenkov radiation. It is extremely unlikely that four liquids with such varying chemical constitutions would give identical fluorescent or phosphorescent emission. The increase in density on going from water and methanol to cyclohexane and benzene can be accounted for by the differences in the refractive indices of these liquids since Cerenkov radiation has a yield which is proportional (to a first approximation) to the inverse of the square of the refractive index. Water and methanol have nearly identical refractive indicies, while the refractive index of cyclohexane is larger than that of water but smaller than that of benzene. Absolute correlation between the emission yields for the four liquids and their refractive indices was not possible since an absolute exposure (i.e. # of photons) was not known and could not be accurately estimated. Qualitatively the agreement was good.

A further significance of these results is that the apparent emission, other than Cerenkov, in the region of 4000 - 4500 Å can not be attributed to a chemical process since it is highly unlikely that the same process would occur in all four liquids. It is possible, however, that the effect may be due to an emission from a physical process of the radiolysis. Possible sources of light emission, due to physical processes, other than Cerenkov radiation are visible Bremsstrahlung and Transition radiation[8]. Bremsstrahlung in the visible region of the electromagnetic spectrum is extremely weak in intensity

and Jelley[8] quotes a relative intensity for Bremsstrahlung as about 10^6 times less than Cerenkov radiation. Transition radiation (radiation produced by electrons at the boundary of two media having different refractive indices) is also known to be of extremely low intensity with a relative intensity of at least four orders of magnitude less than Cerenkov[8]. Thus unless some radiation intensity effect caused an increase in the yield of either of these sources of light, their contribution to the emission should have been negligible.

9. Calculation of a G-value

An estimation of the total photon yield was made in order to confirm the findings of the preceding sections. This was done using the calibrated quartz-iodine lamp, which had a known intensity, and the grating spectrograph. An exposure of the emission from the standard lamp at a known distance from the slits of the spectrograph was made for a fixed length of time. Under identical conditions, and using the same piece of film, the light emission from a number of pulses of water was recorded. A comparison of the densities of the water emission band and the standard lamp emission band was made for the wavelength region 4000 - 5000 Å in order to estimate the relative number of photons. This was done by comparing the relative densities of the two bands with a number of other exposures made on the same piece of film for a progressive series of water experiments where 2, 4, 6, 8 ••• pulses had been given. In this

manner the relative number of photons was estimated to be 2.5 ± 0.5 times in favour of the quartz -iodine lamp which had been exposed for 0.8 milliseconds and for the emission from 12 pulses of water. The photon yield was then calculated as follows:

- The integrated intensity of the standard lamp over the range from 4000 - 5000 Å was 130 μwatts cm.$^{-2}$ at 40 cm.

- Since 2.5 ± 0.5 times as many photons were emitted by the standard lamp as compared to 12 pulses from water, one pulse of water was therefore equivalent to 1/30 of the number of photons from the standard lamp.

- The total amount of energy emitted by the lamp per cm.^{2} at 40 cm. in 0.8 milliseconds was 130×10^{-6} watts cm.$^{-2}$ $\times 8 \times 10^{-4}$ seconds = 1.04×10^{-7} joules cm.$^{-2}$.

- Thus the total amount of energy emitted per cm.^{2} at 40 cm. by the water for 1 pulse of electrons was $0.04 \times 10^{-7}/30$ = 3.5×10^{-9} joules cm.$^{-2}$.

- Assuming the light was emitted isotropically, the total energy emitted by the water was then $4\pi \times 40^2 \times 3.5 \times 10^{-9}$ joules = 4.4×10^{14} eV. since the solid angle formed by 1 cm.^{2} area at 40 cm. is $1/40^2$ steradians and isotropic radiation is emitted equally over a solid angle of 4π steradians.

- Since the average energy of the photons in the region 4000 - 5000 Å is 2.8 eV., the photon yield is then $4.4 \times 10^{14}/2.8 = 1.6 \times 10^{14}$ photons per pulse.

- Using the known radiation dose of 0.9×10^{19} eV. per

pulse gives a G value of $G_{h\nu(4\text{-}5000\,\text{Å})} = 1.8 \times 10^{-3}$.

This discussion has made the assumption that the radiation was emitted isotropically. Cerenkov radiation however would be emitted preferentially in the forward direction, mainly in a cone of $\sim 65^{o}$, and when this is taken into account a G value of about $G_{h\nu(4\text{-}5000\,\text{Å})} \sim 6 \times 10^{-4}$ is obtained.

No error estimations have been included in the calculation since they are difficult to estimate. The largest errors are introduced by the angular distribution and the relative number of photons estimation. A conservative estimate of the uncertainty in the G value would be 60% although the number of photons calculation is probably uncertain by only about 30%.

The photon yield calculated in this work agrees reasonably well with the yield expected for Cerenkov radiation. From formula (xii) it was calculated that about 4 photons per electron would be emitted in the spectral range 4000 - 5000 Å. Using the measured number of electrons 2×10^{13} per pulse, the calculated photon yield is 0.8×10^{14} photons per pulse, which compares favourably with the estimated actual photon yield of 1.6×10^{14} photons.

10. Conclusion

In conclusion, the main finding of this investigation has been that at least 90% of the light emission from water irradiated with an intense pulse of high energy electrons can be attributed to Cerenkov radiation. The yield of the Cerenkov radiation was found to be $G_{h\nu(4\text{-}5000\,\text{Å})} \sim 6 \times 10^{-4}$.

This conclusion was drawn on the basis of; (i) the angular dependence which indicated that the light was predominately in the forward direction; (ii) the variation of the emission intensity with electron energy and the cutoff of emission at ~240 KV electron energy; (iii) the spectrum which showed the expected c/λ^2 vs λ variation; (iv) the effect of additives; (v) the comparison of the emission to emission from other liquids; and (vi) the photon yield which agreed with the expected Cerenkov yield.

It is evident from this work that any light emission from water would have a yield of $G_{h\nu}(\text{visible}) \leqslant 6 \times 10^{-5}$ and thereby indicate that it was the result of an unimportant radiation-chemical process.

The conclusion is also in good agreement with the results of previous work using different radiation sources with the exception of the work of Sitharamareo and Duncan[20] which it appears to contradict. Since they give only a very sketchy outline of their procedure for determining the emission spectra and photon yield, it is not possible to give any explanation of the conflict between this work and theirs.

11. Suggestions for Further Study

The fact that water apparently emitts relatively little light, other than Cerenkov radiation, suggests that a very efficient means of energy degradation must exist in the liquid. Some suggestions for further study would therefore include an attempt to scavenge some of the energy by adding an efficient

energy absorber, such as anthracene, to the water; observing the fluorescence from ice or glassy water and possibly looking for fluorescence from water vapour, where Cerenkov radiation would be nonexistent because of the small refractive index.

REFERENCES

1. J.W.T. Spinks and R.J. Woods, An Introduction to Radiation Chemistry, John Wiley & Sons, New York, 1964, p.39.

2. J.W.T. Spinks and R.J. Woods, op. cit., pp. 15-76.

3. I.V. Vershchinskii and A.K. Pikaev, Introduction to Radiation Chemistry, English Translation from Israel Program for Scientific Translations, Jerusalem, 1964, pp. 6-16.

4. G.J. Hine and G.L. Brownell, ed., Radiation Dosimetry, Academic Press, New York, 1956, pp. 153-528.

5. I.V. Vershchinskii and A.K. Pikaev, op. cit., p. 12.

6. A.O. Allen, The Radiation Chemistry of Water and Aqueous Solutions, D. Van Nostrand, New York, 1961.

7. E. Collinson, Annual Report of Progress in Chemistry (Chemical Society, London) 62, 79-105, 1965.

8. J.V. Jelley, Cerenkov Radiation, Pergamon Press, London, 1958.

9. L. Mallet, Compt. Rend. Acad. Sci. (Paris) 183, 274, 1926.

10. P.A. Cerenkov, Dokl. Akad. Nauk, SSSR, 2, 451, 1934.

11. I.M. Frank and I. Tamm, Dokl. Akad. Nauk, SSSR, 14 (3), 109, 1937.

12. R.E. Jennings, Science Progress, 50, 364, 1962.

13. G.B. Collins and V.G. Reiling, Physical Review, 54, 499, 1938.

14. M.A. Greenfield, A. Norman, A.H. Drowdy and P.M. Dratz, J. Opt. Soc. Am., 43 (1), 42, 1953.

15. J.A. Rich, R.E. Slovacek and F.J. Studer, J. Opt. Soc. Am., 43 (9),750, 1953.

16. E.H. Belcher, Proc. Roy. Soc., A216, 90, 1953.

17. E.W.T. Richards, Proc. Phys. Soc., A67, 922, 1953.

18. L.O. Brown and N. Miller, Trans Faraday Soc., 51, 1623, 1955.

19. E.W.T. Richards, AERE Harwell, C/R 1901, 1956.

20. D.N. Sitharamarao and J.F. Duncan, J. Phys. Chem., 67, 2126, 1963.

21. G. Czapski and D. Katakis, J. Phys. Chem., 70, 637, 1966.

22. D.C. Walker, Quart. Rev., 21 (1), 79, 1967.

23. D.C. Walker, Private Communication.

24. O. Oldenberg and F.F. Rieche, J. Chem. Phys., 17, 485, 1939.

25. C.D. Hodgman, ed., Handbook of Chemistry and Physics, The Chemical Rubber Publishing Co., Cleveland, Ohio, 44th edition, 1962, p. 2698.

26. D.A. Head, Private Communication.

27. E.J. Henley, Nucleonics, 12 (9), 62, 1954.

28. R.C.A. Phototubes and Photocells - Technical Manual PT-60, R.C.A. Victor Company, Ltd., Montreal, 1963.

29. A.M. Bass and K.G. Kessler, J. Opt. Soc. Am., 49, 1223, 1959.

30. C.A. Parker, Proc. Roy. Soc., A220, 104, 1953.

31. C.G. Hatchard and C.A. Parker, Proc. Roy. Soc., A235, 518, 1956.

32. K. Kawabata and S. Okabe, Osaka Furitso Hoshawen Chuo Kinkujo Saki, Japan, 6, 71, 1965.

33. T.H. James, ed., The Theory of the Photographic Process, 3rd edition, The Macmillan Company, New York, 1966.

Fig. 2

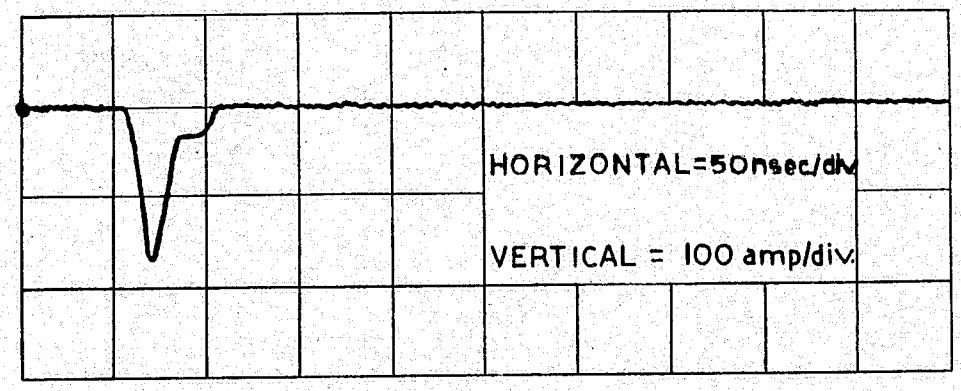
HORIZONTAL=50nsec/div.
VERTICAL = 100 amp/div.

(a)

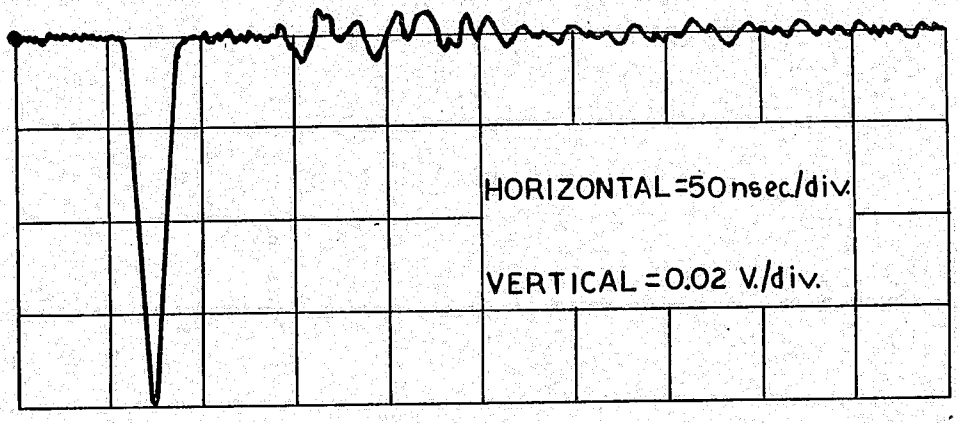
HORIZONTAL=50nsec/div.
VERTICAL =0.02 V./div.

(b)

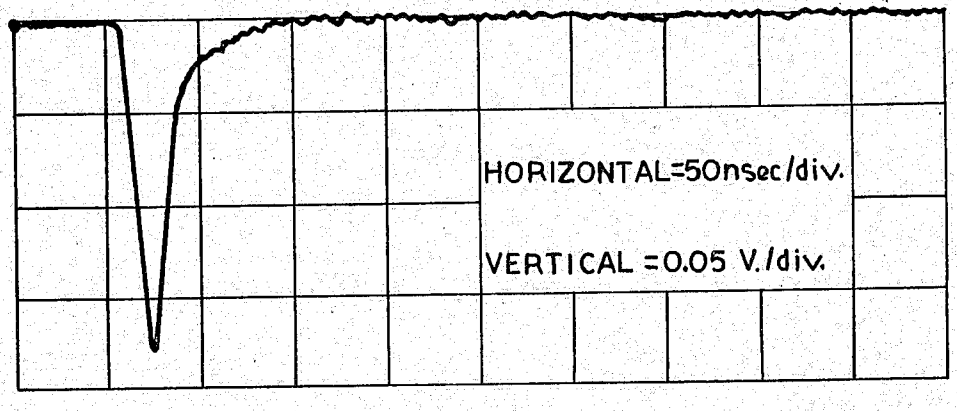
HORIZONTAL=50nsec/div.
VERTICAL =0.05 V./div.

(c)

Fig. 3

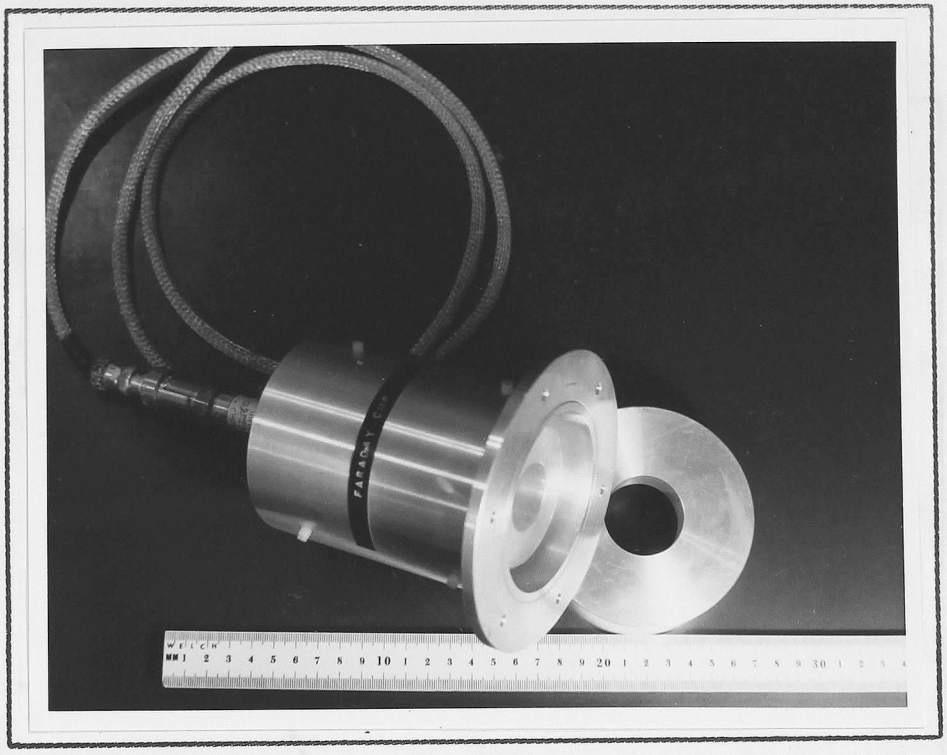

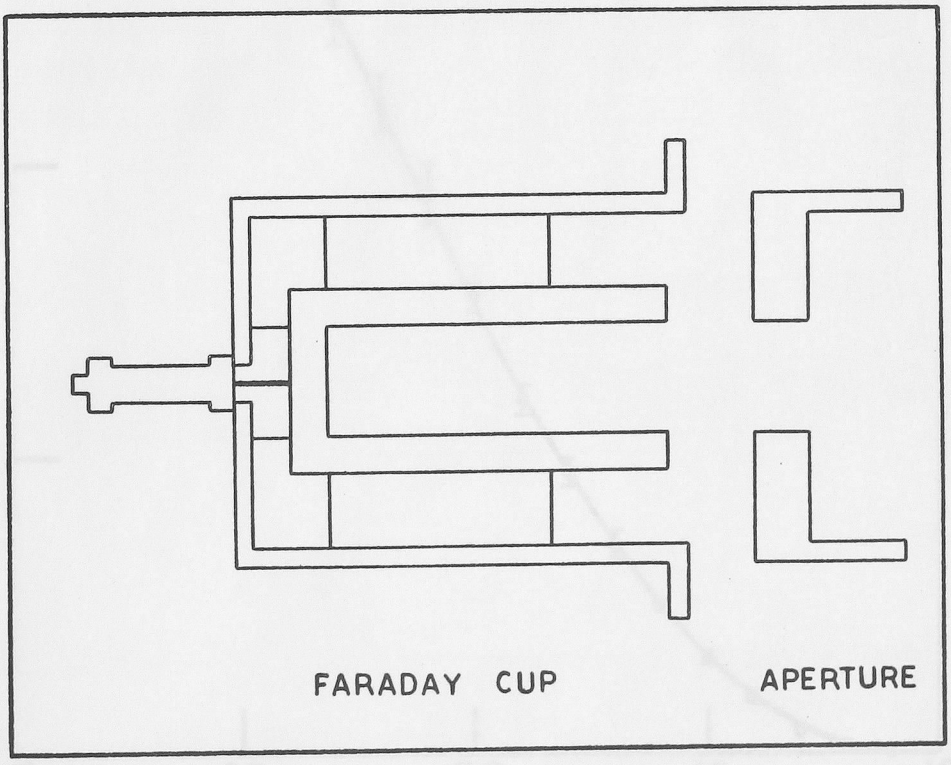

Fig. 4

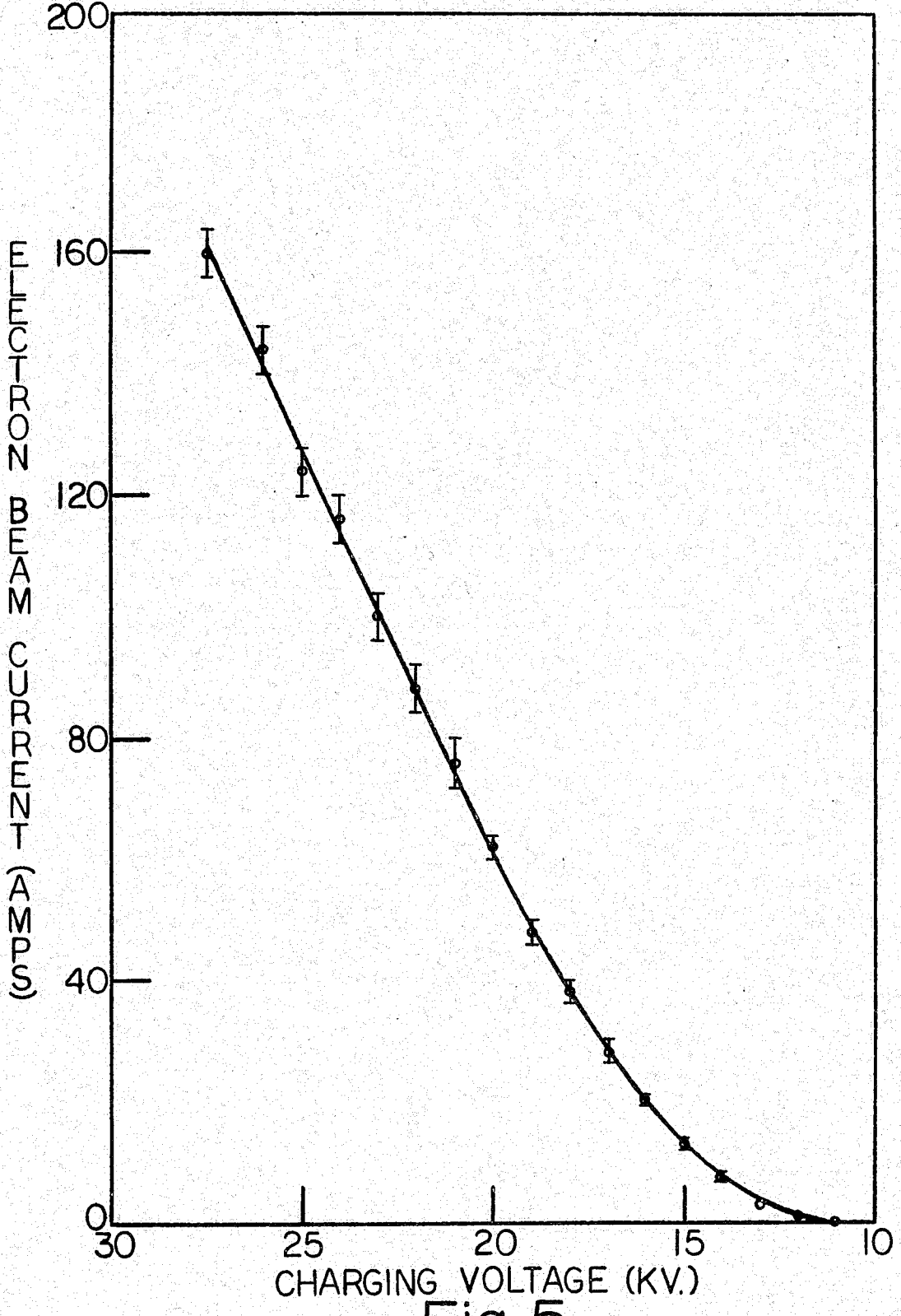
200
160
120
80
40
0
ELECTRON BEAM CURRENT (AMPS)
30
25
20
15
10
CHARGING VOLTAGE (KV.)

Fig. 5

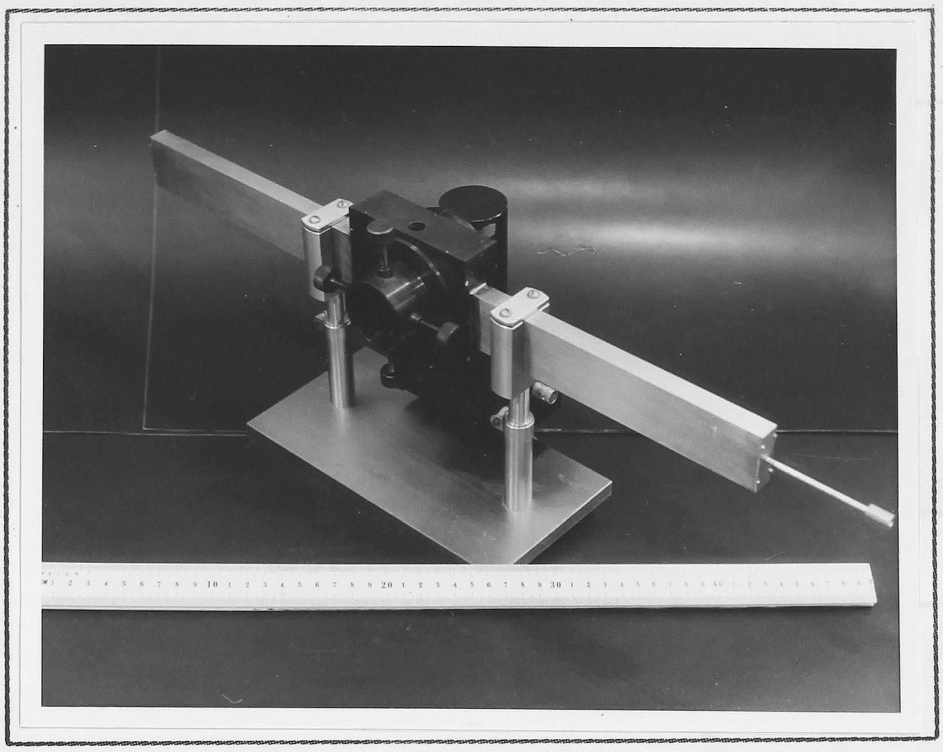

(a)

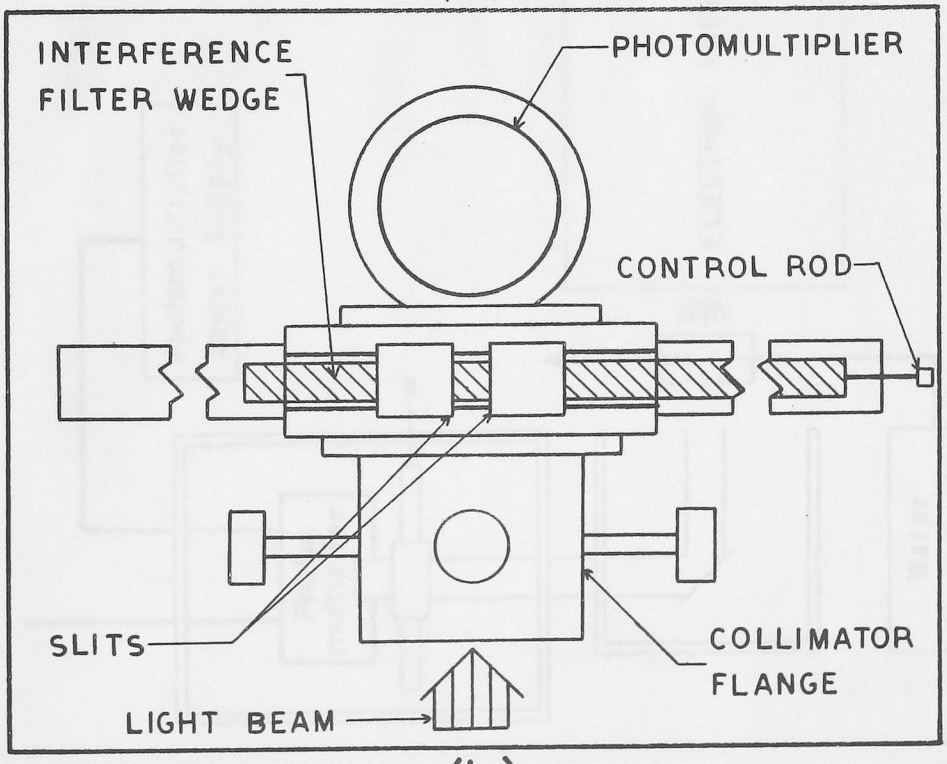
INTERFERENCE
FILTER WEDGE
PHOTOMULTIPLIER
CONTROL ROD
SLITS
COLLIMATOR
FLANGE
LIGHT BEAM

(b)

Fig. 6

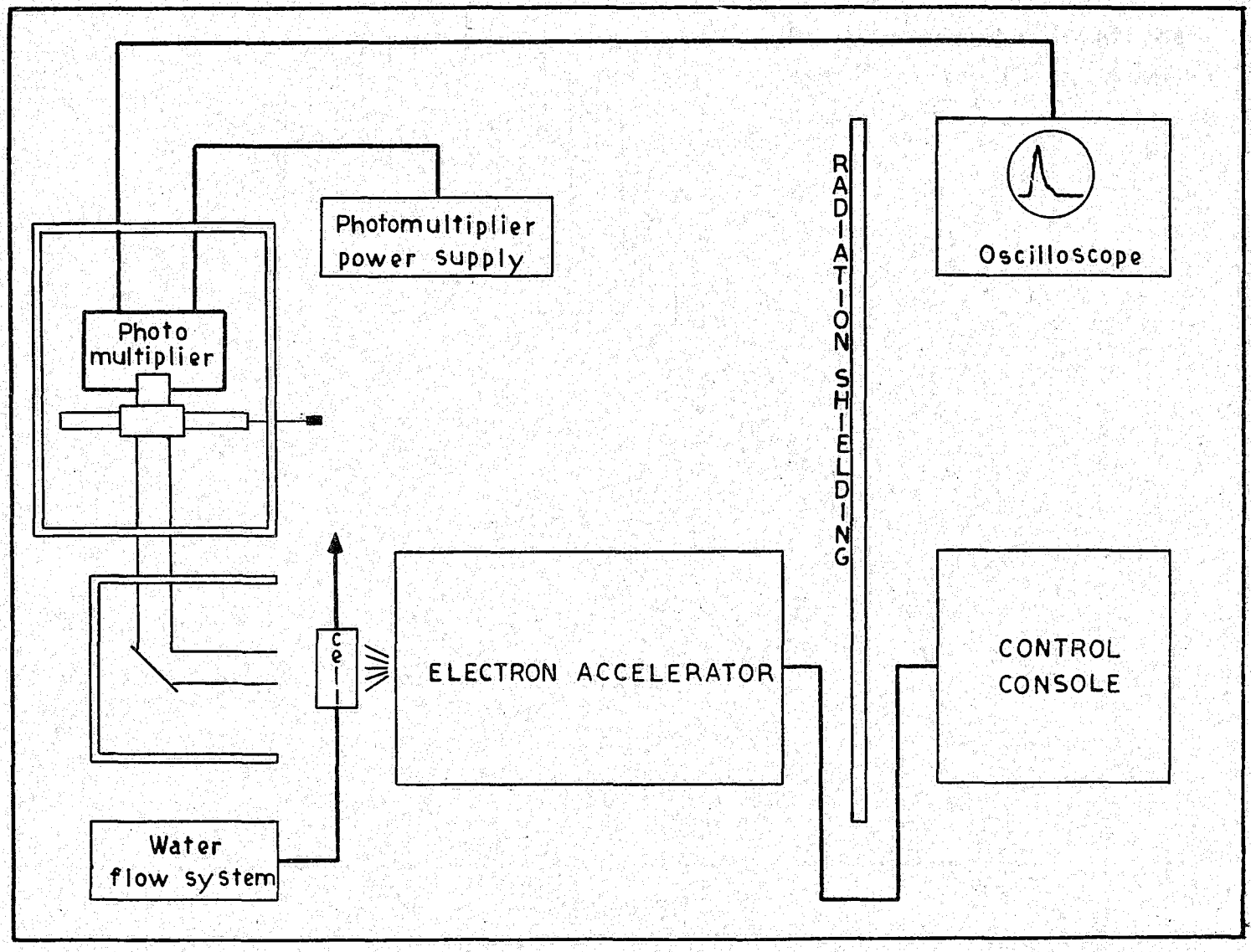
Photomultiplier
power supply
Oscilloscope
Photo
multiplier
RADIATION SHIELDING
ELECTRON ACCELERATOR
CONTROL
CONSOLE
Water
flow system

Fig. 7

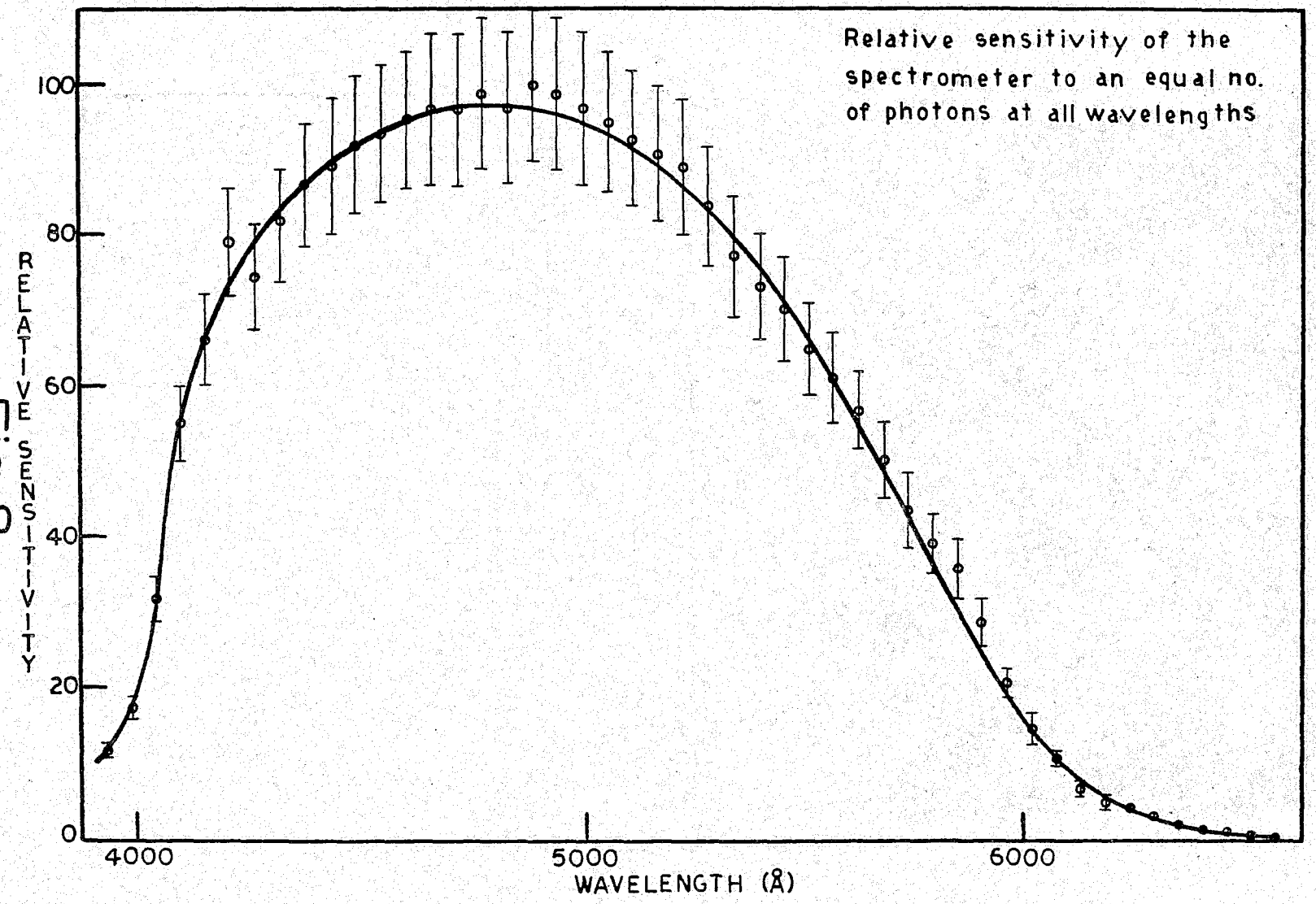
Relative sensitivity of the spectrometer to an equal no. of photons at all wavelengths
RELATIVE SENSITIVITY
100
80
60
40
20
0
4000
5000
6000
WAVELENGTH (Å)

Fig. 8

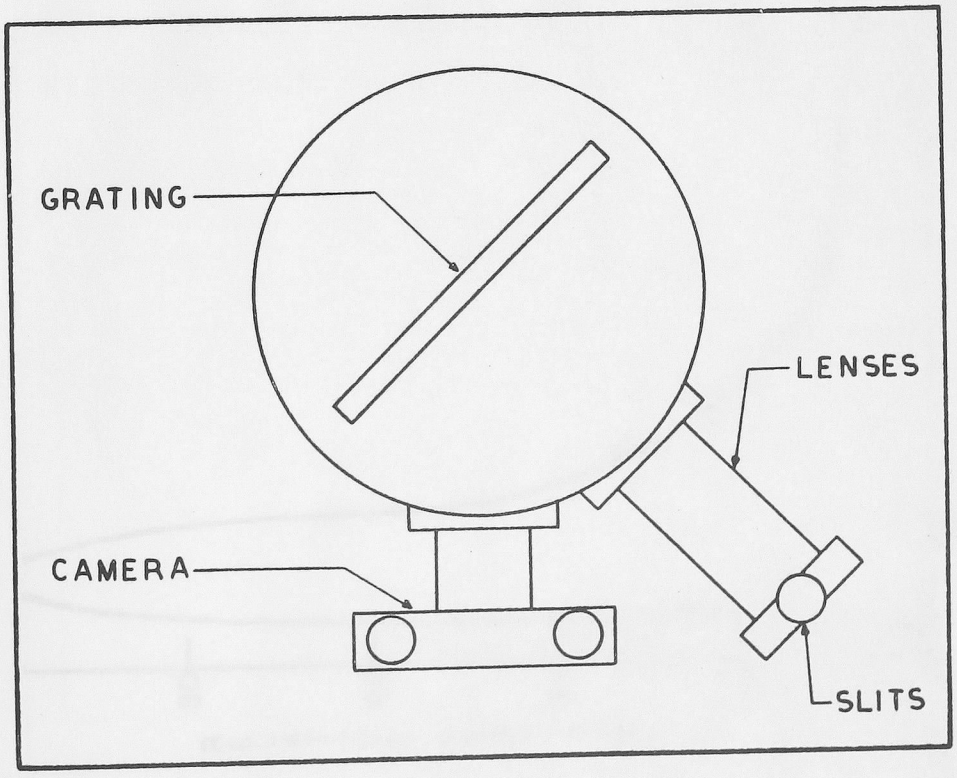

Fig.9

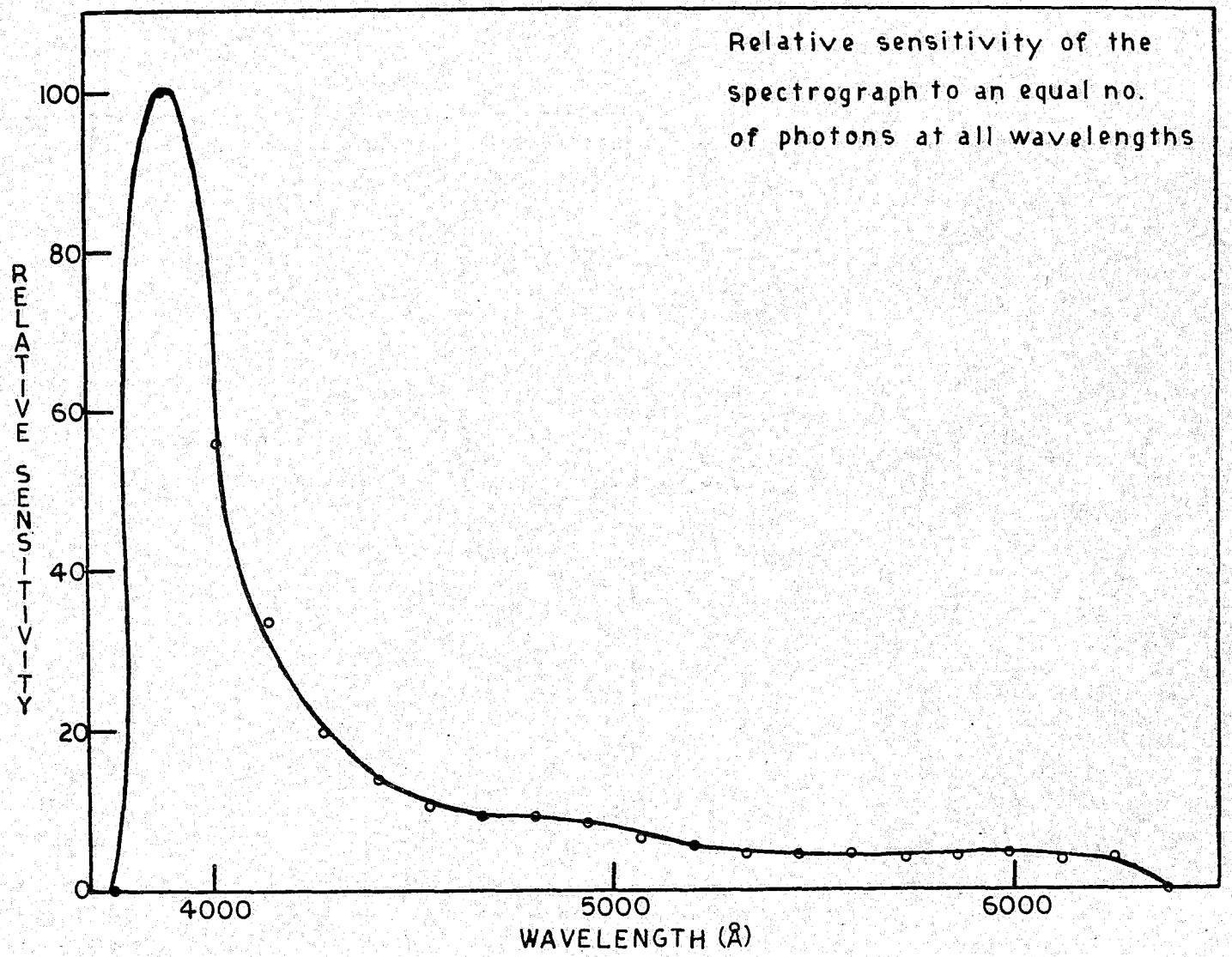
Relative sensitivity of the spectrograph to an equal no. of photons at all wavelengths
RELATIVE SENSITIVITY
100
80
60
40
20
0
4000
5000
6000
WAVELENGTH (Å)

Fig.10

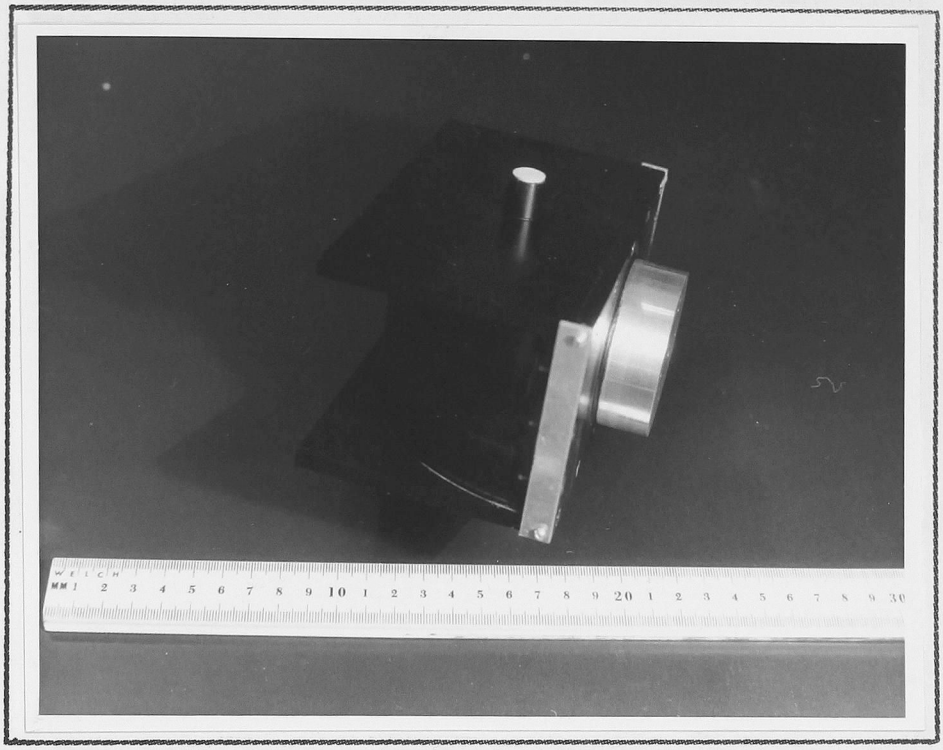

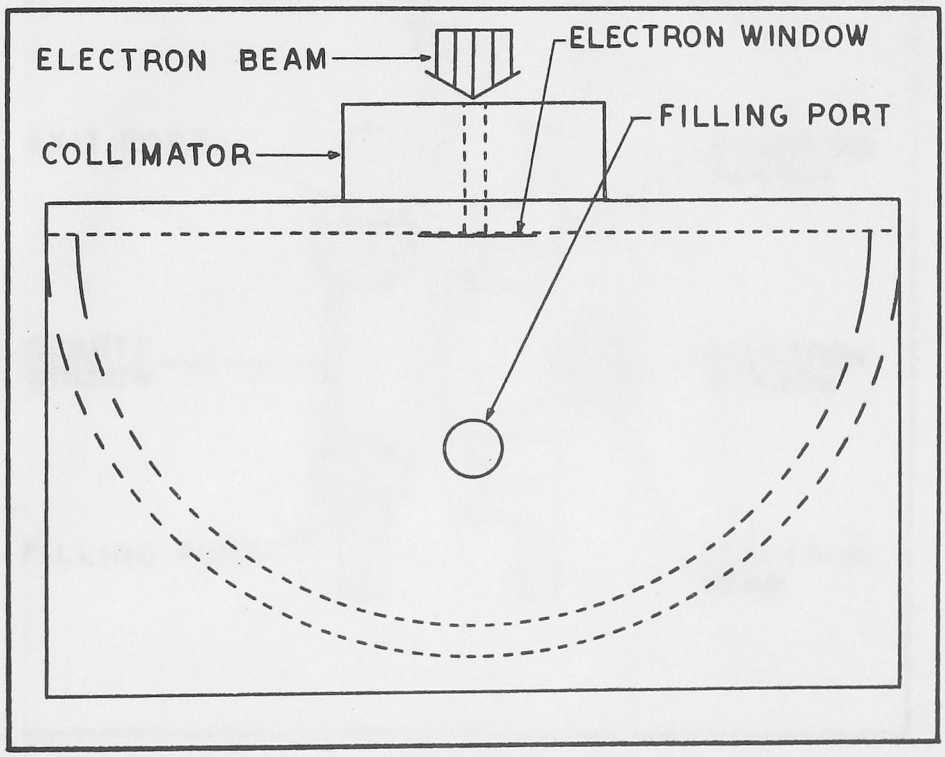

Fig.11

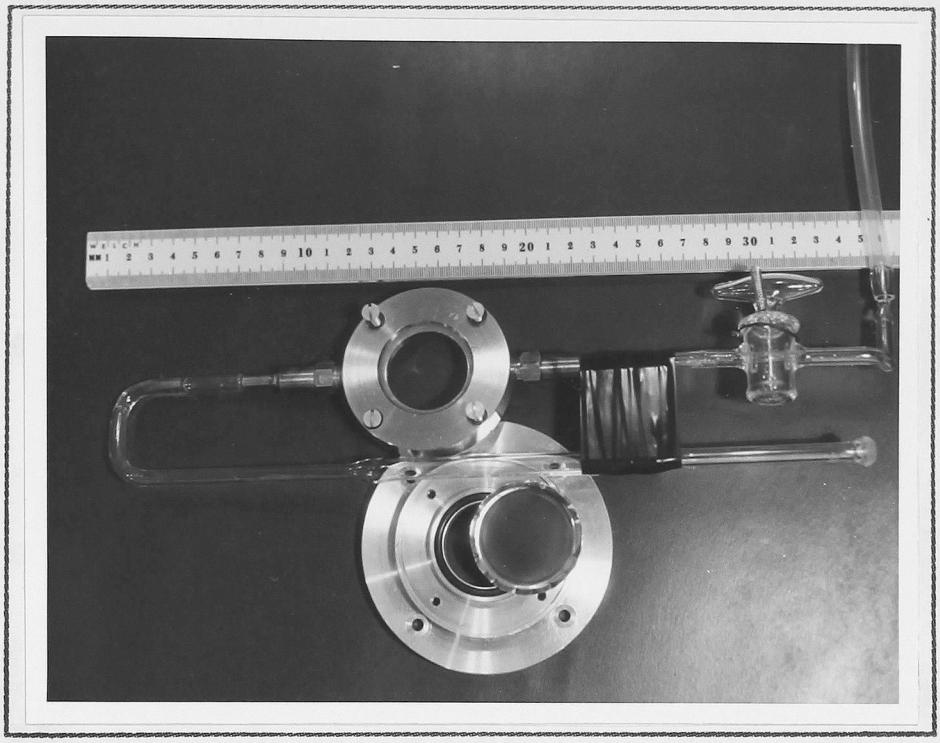

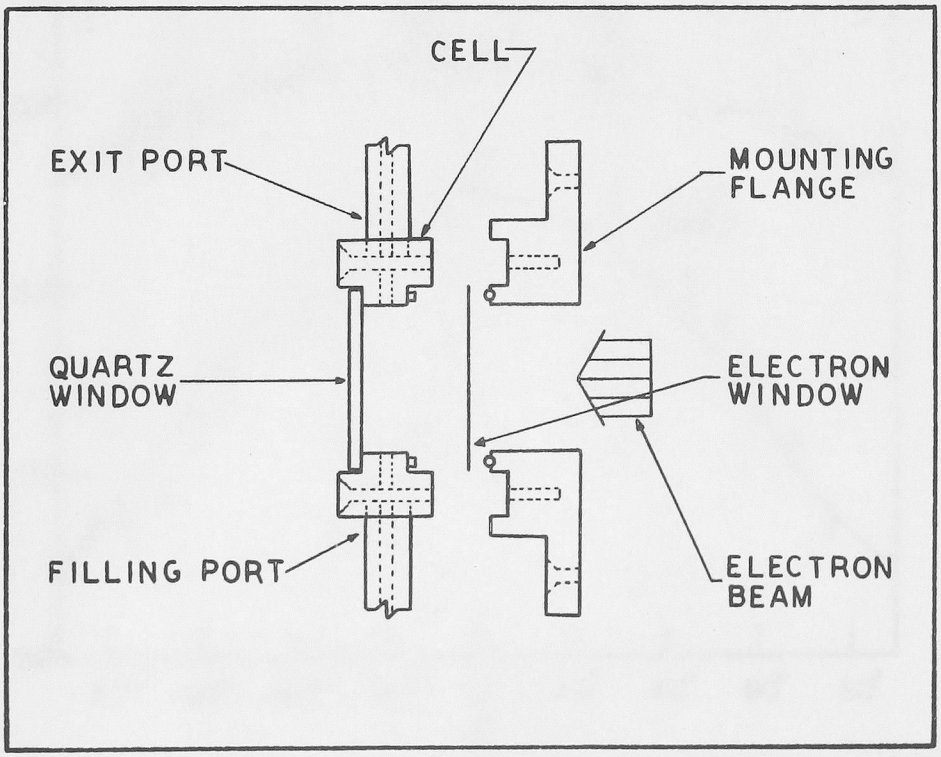
CELL
EXIT PORT
MOUNTING FLANGE
QUARTZ WINDOW
ELECTRON WINDOW
FILLING PORT
ELECTRON BEAM

Fig.12

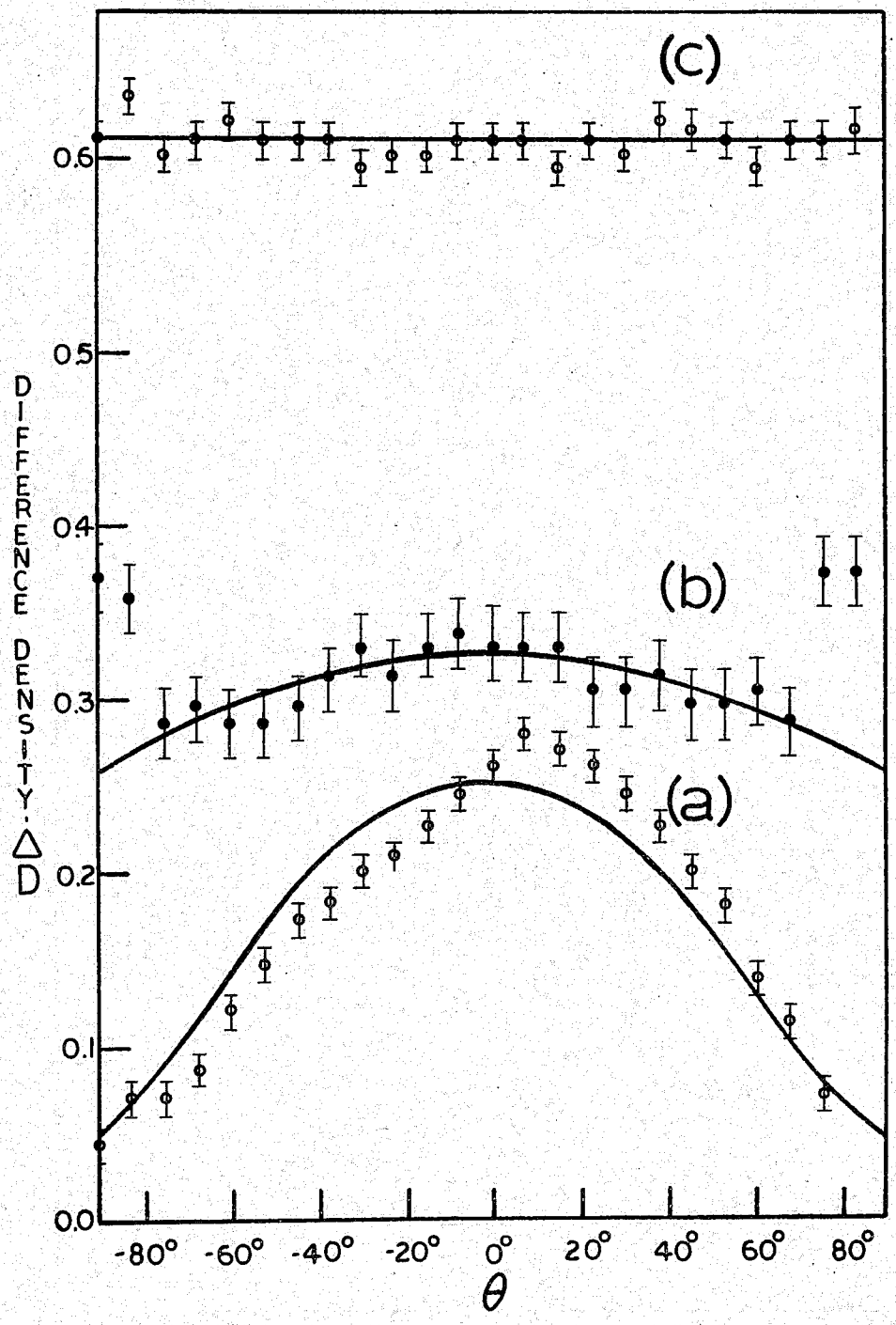
(c)
(b)
(a)
0.6
0.5
0.4
0.3
0.2
0.1
0.0
DIFFERENCE DENSITY-ΔD
-80°
-60°
-40°
-20°
0°
20°
40°
60°
80°
θ

Fig.13

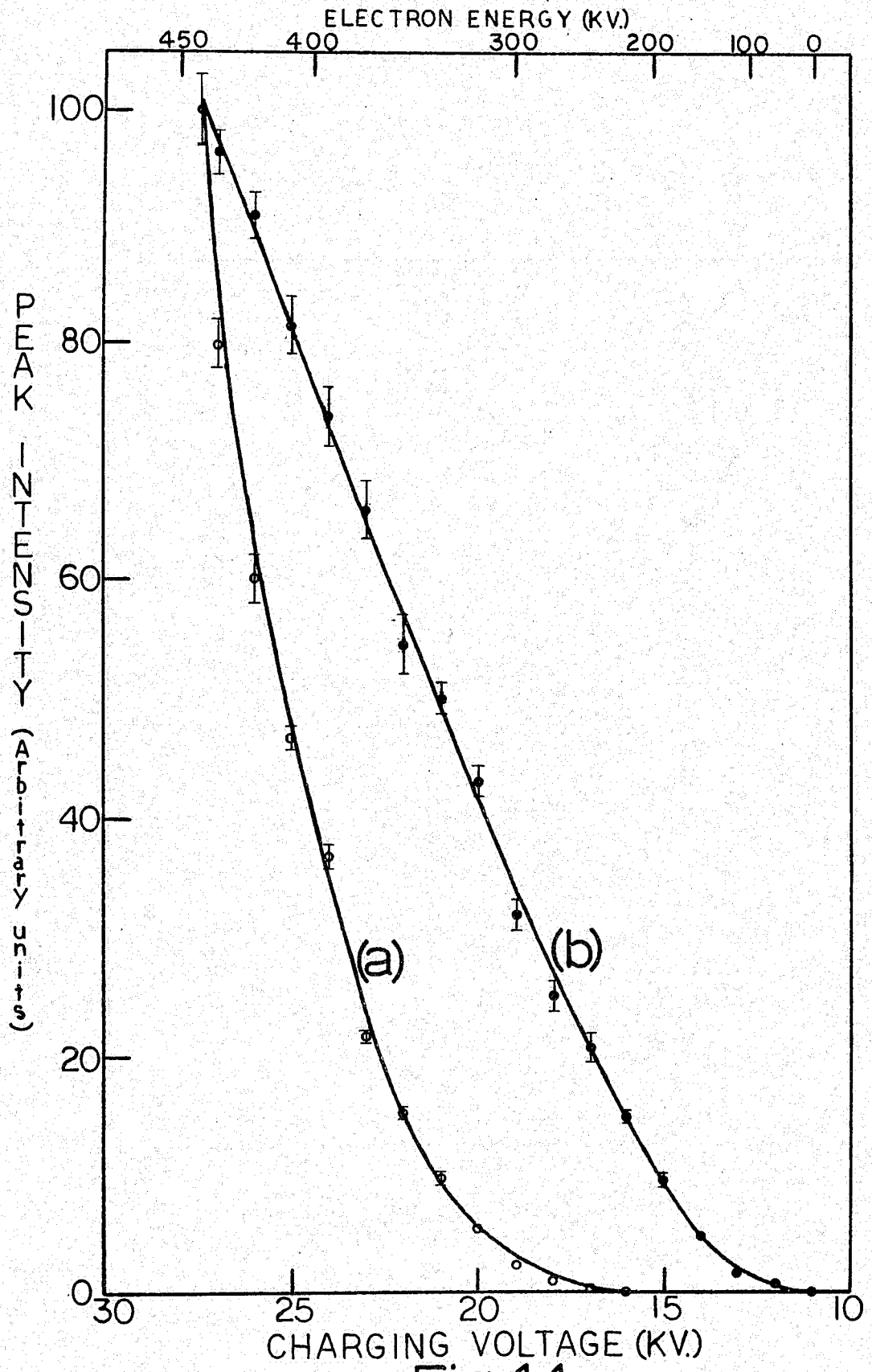
ELECTRON ENERGY (KV.)
450
400
300
200
100
0
100
80
60
40
20
0
PEAK INTENSITY (Arbitrary units)
(a)
(b)
30
25
20
15
10
CHARGING VOLTAGE (KV.)

Fig. 14

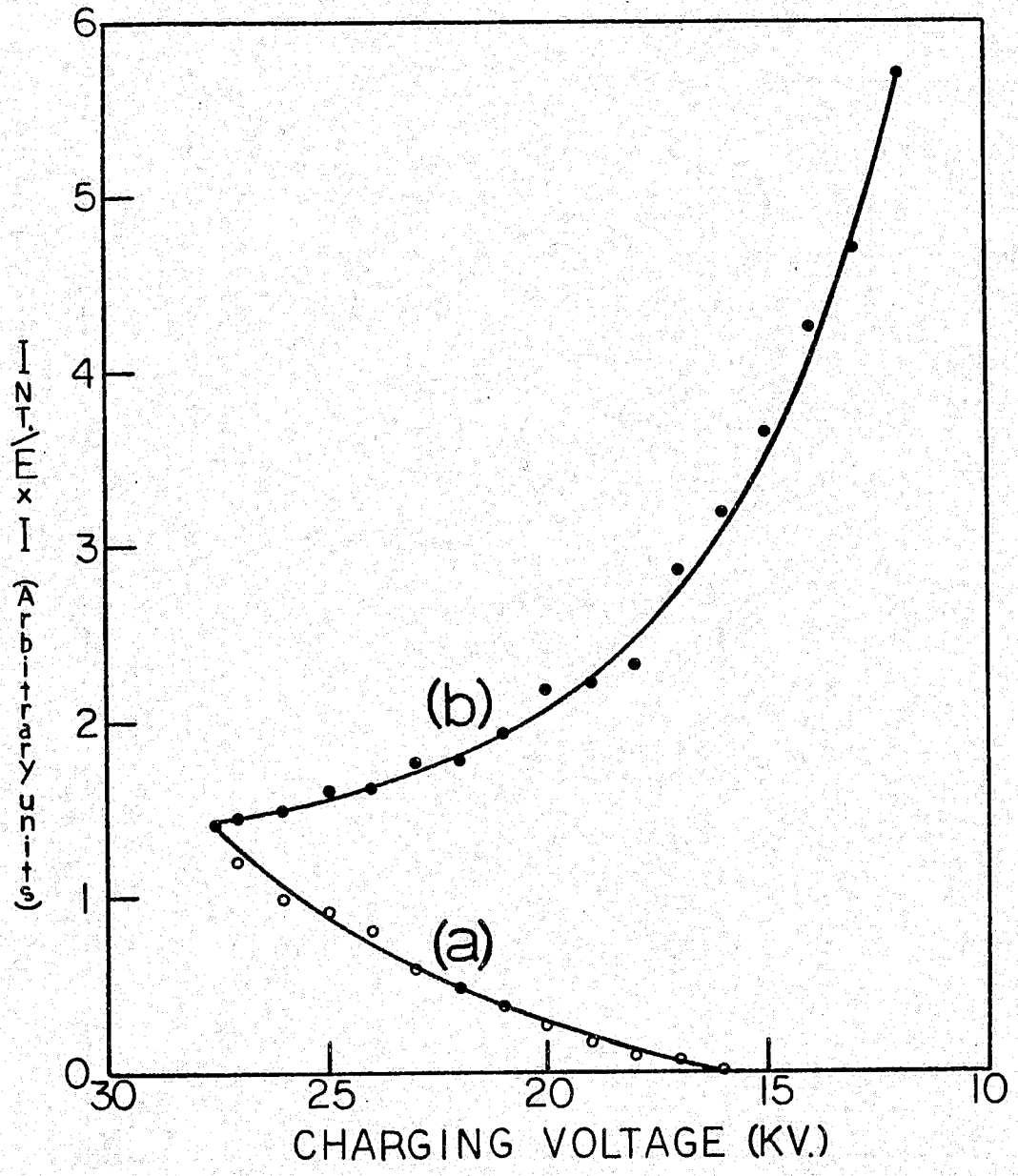
6
5
4
3
2
1
0
INT. \E x I (Arbitrary units)
(b)
(a)
30
25
20
15
10
CHARGING VOLTAGE (KV.)

Fig.15

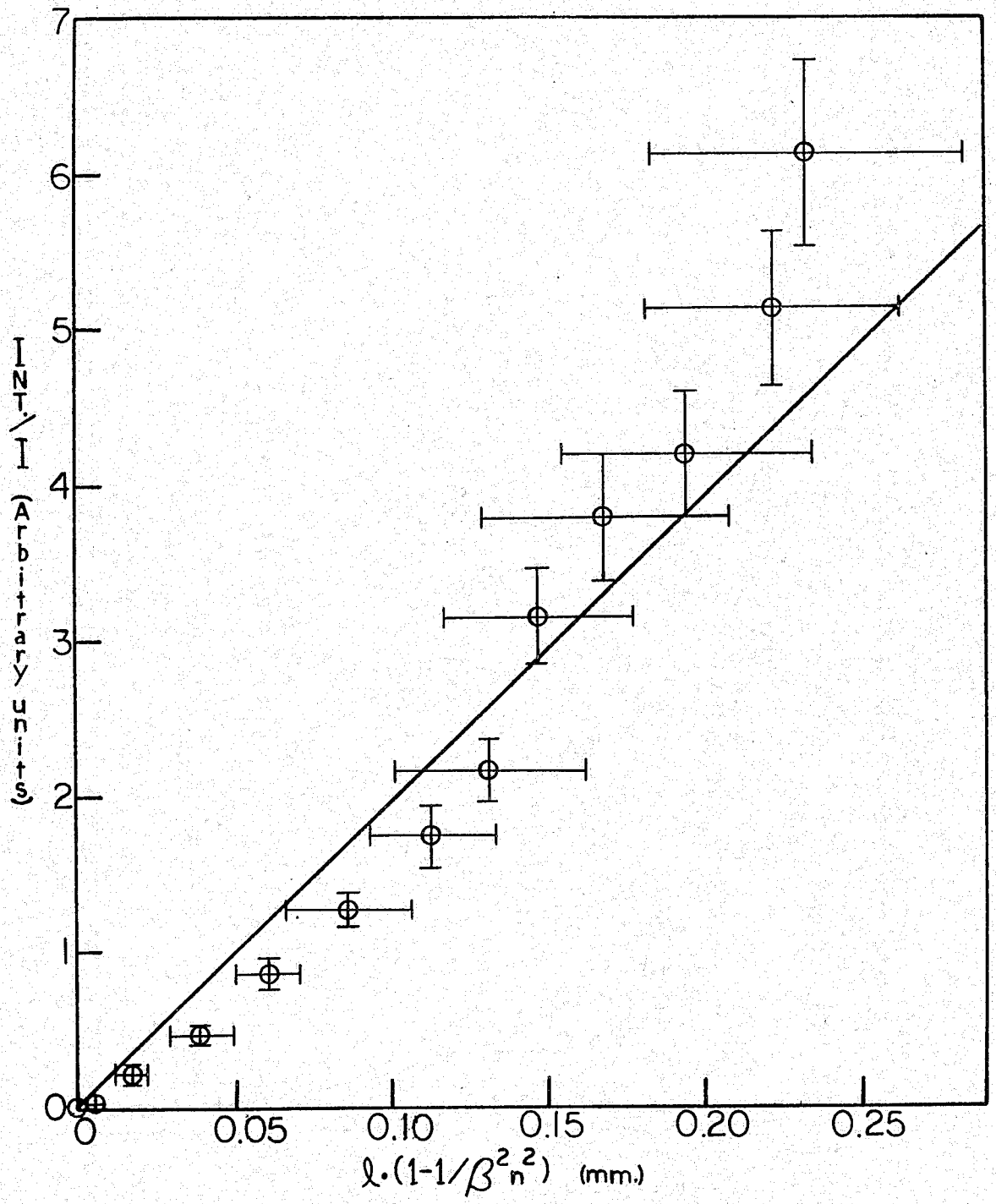
7
6
5
4
3
2
1
0
INT./I (Arbitrary units)
0
0.05
0.10
0.15
0.20
0.25
l·(1-1/β²n²) (mm.)

Fig.16

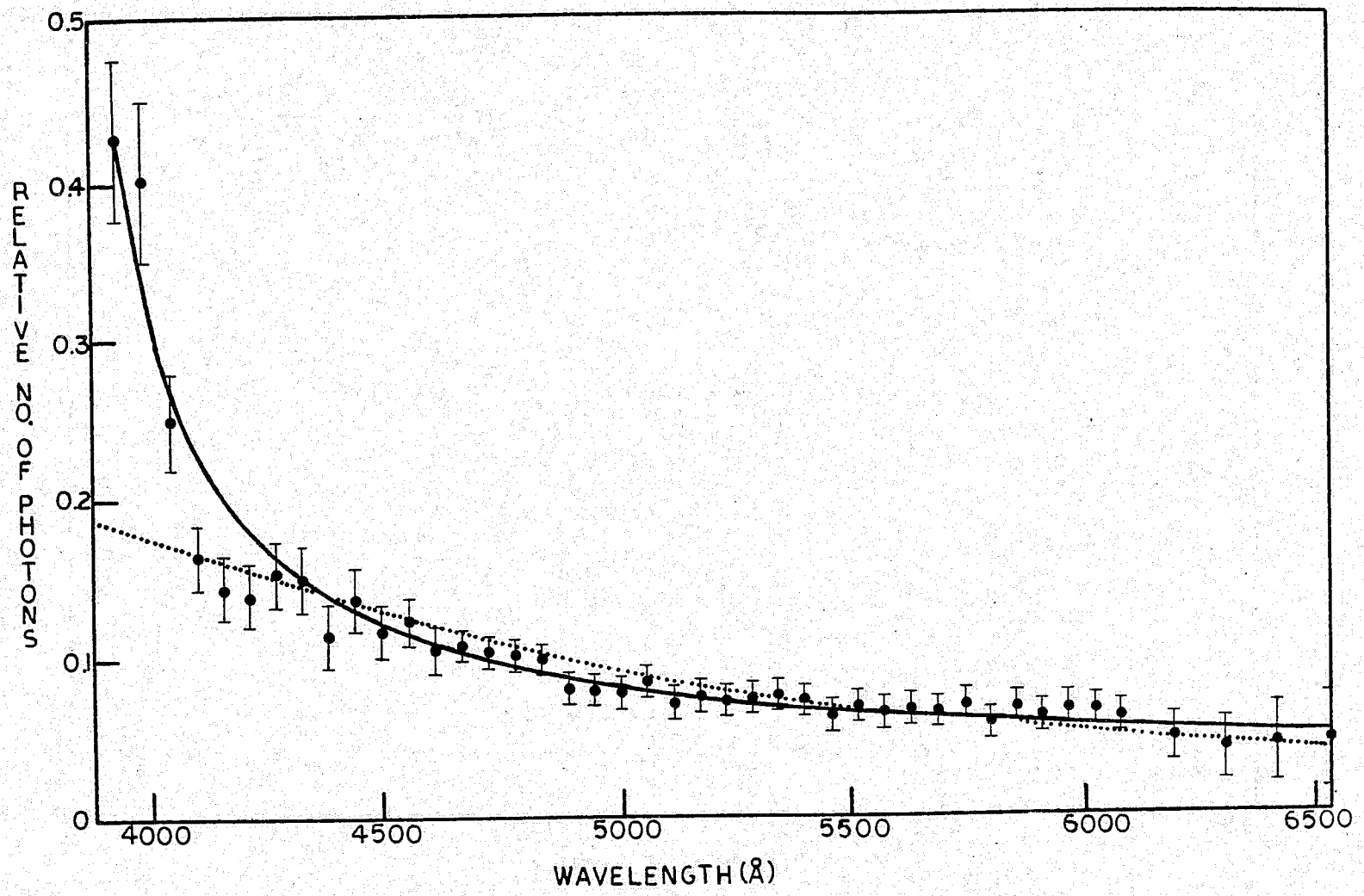
0.5
0.4
0.3
0.2
0.1
0
RELATIVE NO. OF PHOTONS
4000
4500
5000
5500
6000
6500
WAVELENGTH (Å)

Fig. 7

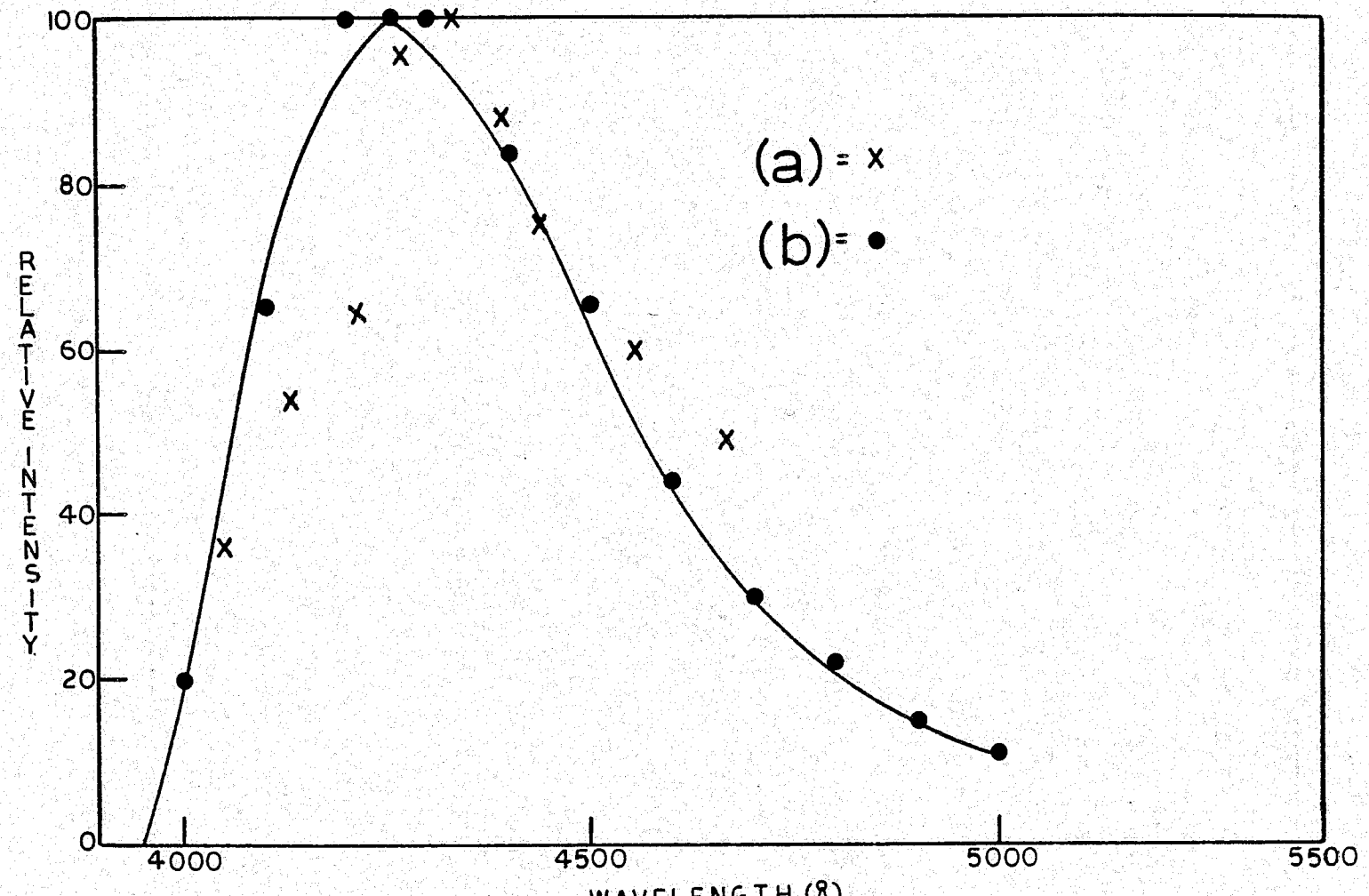
100
80
60
40
20
0
RELATIVE INTENSITY
4000
4500
5000
5500
WAVELENGTH (Å)
(a) = x
(b) = ●

Fig.18

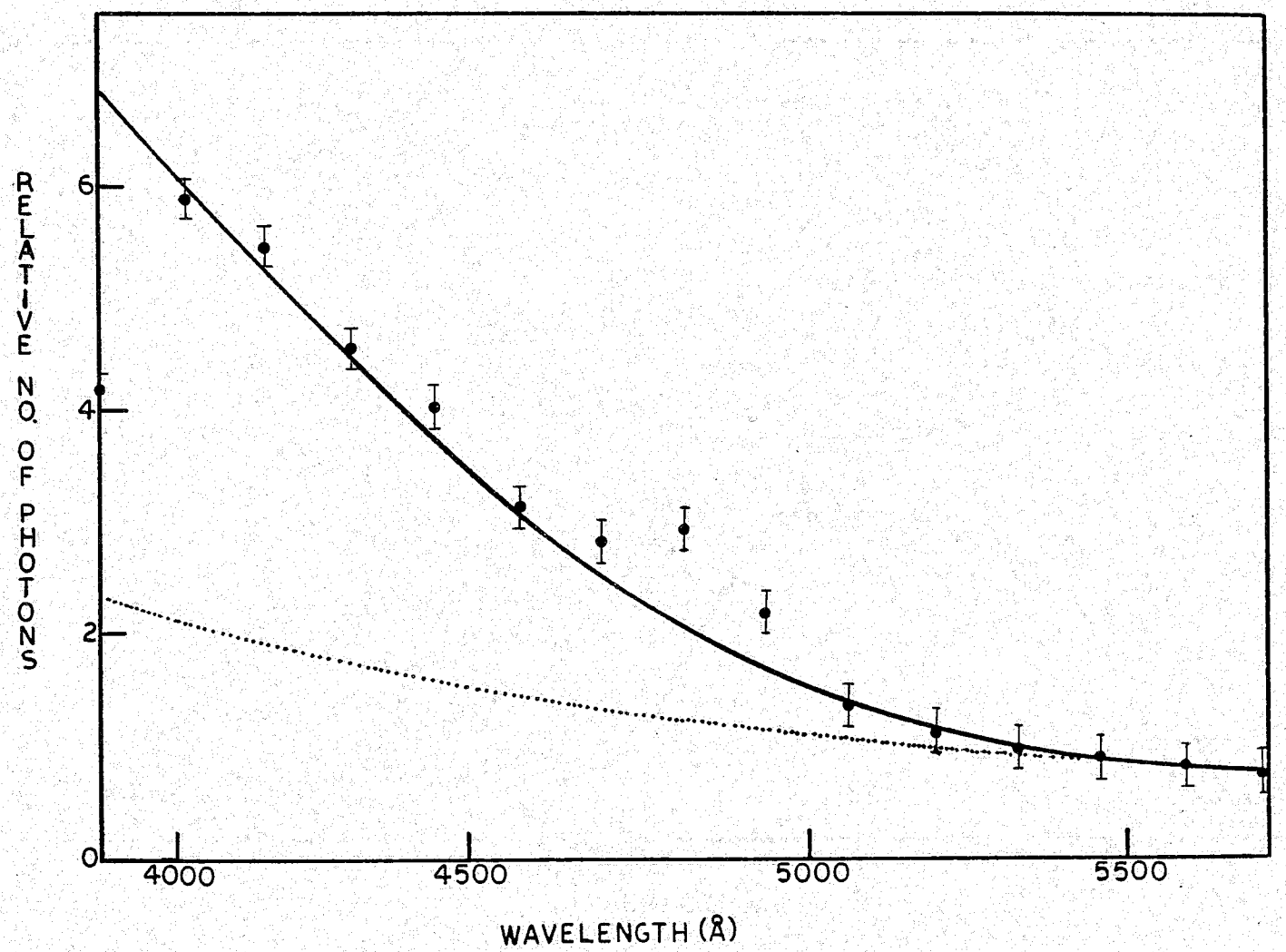
RELATIVE NO. OF PHOTONS
0
2
4
6
4000
4500
5000
5500
WAVELENGTH (Å)

Fig.19

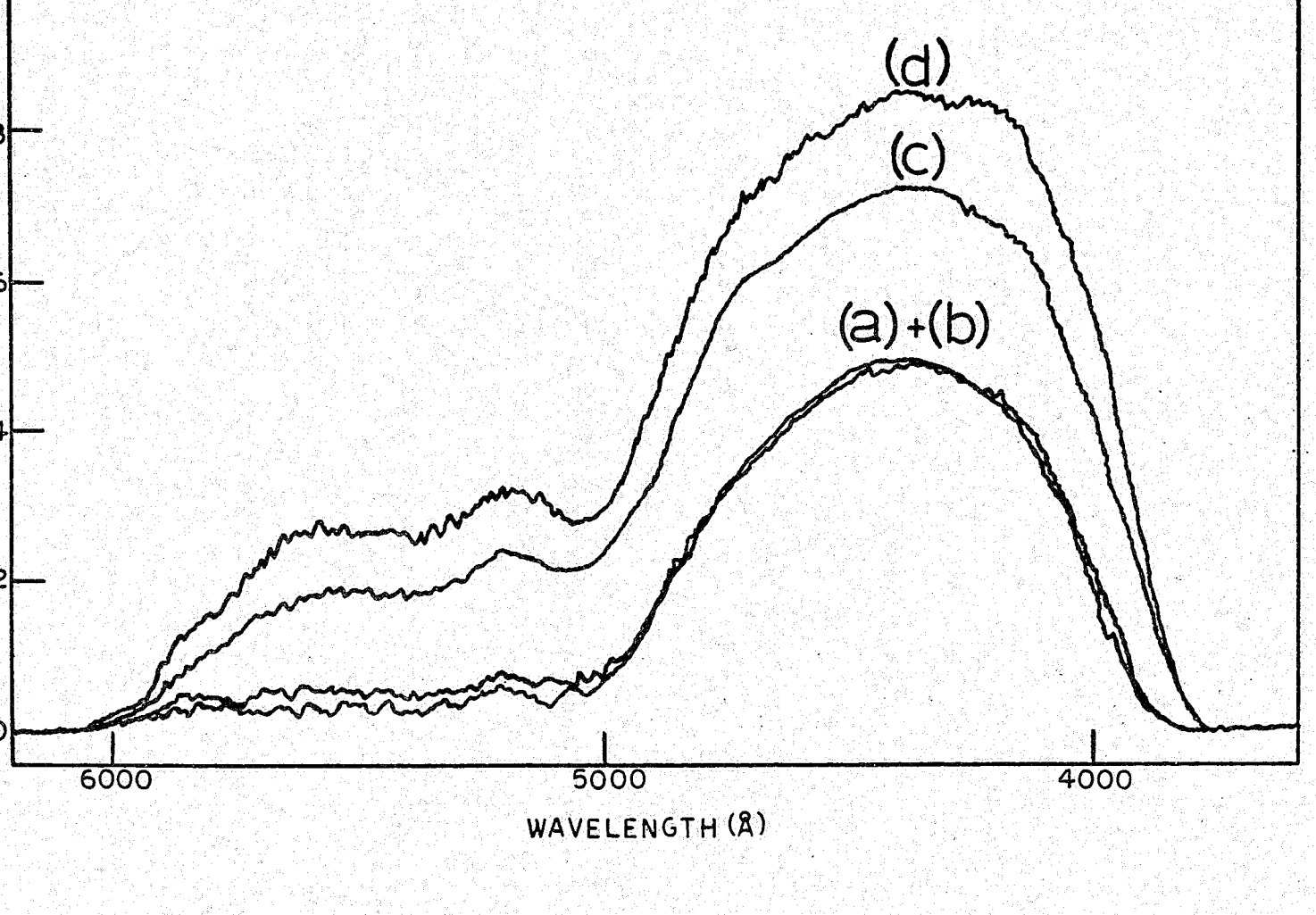

Fig. 20

ADDENDUM

The fact that the graph in Fig.16 appears to be a curve rather than a straight line is most likely due to an error in the expression used for the number of photons emitted by an electron. The expression derived in the theory of Frank and Tamm[11],

$$N = 2\pi\alpha l \left(\frac{1}{\lambda_2} - \frac{1}{\lambda_1}\right)\left(1 - \frac{1}{\beta^2 n^2}\right)$$

was obtained using the assumption that the electrons' velocity is constant during its passage through the medium. However, in actual fact, β does change markedly as the electron penetrates into the water. This can be taken into account by using an expression for the linear energy transfer to the medium by the electrons to relate β to l in the following manner:

$$dl = \frac{-\beta^2 dE}{K}$$

where dE is the increment of energy loss and K is a constant. dE is related to $d\beta$ by an expression of the form:

$$dE = m_o c^2 \beta \left(\frac{1}{1-\beta^2}\right)^{3/2} d\beta$$

where $m_o c^2$ is the rest energy of the electron. Hence the expression for dl becomes:

$$dl = -\beta^3 \left(\frac{1}{1-\beta^2}\right)^{3/2} \frac{m_o c^2}{K} d\beta$$

Including this in the expression for the number of photons emitted per unit path;

$$\frac{dN}{dl} = 2\pi\alpha \left(\frac{1}{\lambda_2} - \frac{1}{\lambda_1}\right)\left(1 - \frac{1}{\beta^2 n^2}\right)$$

results in the following expression:

$$dN = A\left(\frac{\beta^2 n^2 - 1}{(1-\beta^2)^{3/2}}\right)\beta \, d\beta$$

where A is a constant equal to $-2\pi\alpha\left(\frac{1}{\lambda_2} - \frac{1}{\lambda_1}\right) m_o c^2 / n^2 K$.

Integration of this expression between the limits ; dN from 0 to N and d β from 1/n to β , gives an expression of the form:

$$N = A\left[\frac{(\beta^2 n^2 - 1)}{(1-\beta^2)^{1/2}} + 2n^2(1-\beta^2)^{1/2} - 2n(n^2-1)^{1/2}\right]$$

A plot of N vs $\frac{(\beta^2 n^2 - 1)}{(1-\beta^2)^{1/2}} + 2n^2(1-\beta^2)^{1/2}$ then gives a line which is much more nearly linear than Fig. 16.

LIST OF CORRECTIONS

Page	Line	Correction
1	5th last	Z^2Z^2/m^2 to read z^2Z^2/m^2
3	1st	extropolated to read extrapolated
3	3rd	mg/cm^z to read mg/cm^2
8	3rd	process to read processes
8	eqn.4	$e^-_{\substack{\text{polarization} \\ \text{thermal of } H_2O}}$ to read $e^-_{\substack{\text{polarization} \\ \text{thermal of } H_2O}}$
13	6th last	expresses to read expressed
15	10th	using sensitive to read using a sensitive
27	5th last	Kodac to read Kodak
29	1st	this converted to read this was converted
33	2nd	Kodac to read Kodak
35	2nd	balnk to read blank
48	6th	methanol cyclohexane to read methanol , cyclohexane